

Spectrally Stable Ink Variability In A Multi-Primary Printer

Edward F. Hattenberger

B.S. SUNY College of Environmental Science and Forestry

(1999)

A thesis submitted in partial fulfillment of the requirements
for the degree of Master of Science in Color Science
in the Chester F. Carlson Center of Imaging Science
of the College of Science,
Rochester Institute of Technology

June 2003

Signature of the Author

Accepted by Dr. Roy S. Berns,
Coordinator, M.S. Degree Program

CENTER FOR IMAGING SCIENCE
ROCHESTER INSTITUTE OF TECHNOLOGY
ROCHESTER, NEW YORK

CERTIFICATE OF APPROVAL

M.S. DEGREE THESIS

The M.S. Degree Thesis of Edward F. Hattenberger
has been examined and approved by the thesis
committee as satisfactory for the thesis
requirement for the Master of Science Degree

Dr. Noboru Ohta, Thesis Advisor

Mitchell Rosen

CENTER FOR IMAGING SCIENCE
ROCHESTER INSTITUTE OF TECHNOLOGY
ROCHESTER, NEW YORK

THESIS REPRODUCTION PERMISSION STATEMENT

Title of thesis: **Spectrally Stable Ink Variability In A Multi-Primary Printer**

I, Edward F. Hattenberger, hereby **grant permission** to the Wallace Library of the Rochester Institute of Technology to reproduce my thesis in whole or in part. Any reproduction will not be for commercial use or profit.

Date: _____ Signature of Author: _____

Spectrally Stable Ink Variability In A Multi-Primary Printer

Edward F. Hattenberger

B.S. SUNY College of Environmental Science and Forestry
(1999)

A thesis submitted in partial fulfillment of the requirements
for the degree of Master of Science in Color Science
in the Chester F. Carleson Center of Imaging Science
of the College of Science,
Rochester Institute of Technology

ABSTRACT

It was shown previously that a multi-ink printer can reproduce spectral reflectances within a specified tolerance range using many distinct ink combinations. An algorithm was developed to systematically analyze a printer to determine the amount of multi-ink variability throughout its spectral gamut. The advantage of this algorithm is that any spectral difference metric can be used as the objective function. Based on the results of the analysis for one spectral difference metric, six-dimensional density map displays were constructed to illustrate the amount of spectral redundancy throughout the ink space. One CMYKGO ink-jet printer was analyzed using spectral reflectance factor RMS as the spectral difference metric and selecting 0.02 RMS as the tolerance limit. For these parameters, the degree of spectral matching freedom for the printer reduced to five inks because the chromatic inks were able to reproduce spectra within the 0.02 tolerance limit throughout the printer's gamut.

Experiments were designed to exploit spectrally stable multi-ink variability within the analyzed printer. The first experiment used spectral redundancy to visually evaluate spectral difference metrics. Using the developed database of spectrally similar samples allows any spectral difference metric to be compared to a visual response. The second experiment demonstrated the impact of spectral redundancy on spectral color management. Typical color image processing techniques use profiles consisting of sparse multi-dimensional lookup tables that interpolate between adjacent nodes to prepare an image for rendering. It was shown that colorimetric error resulted when interpolating between lookup table nodes that were inconsistent in digital count space although spectrally similar. Finally, the analysis was used to enable spectral watermarking of images. To illustrate the significance of this watermarking technique, information was embedded into three images with varying levels of complexity. Prints were made verifying that information could be hidden while preserving the visual and spectral integrity of the original image.

Spectrally Stable Ink Variability In A Multi-Primary Printer

Edward F. Hattenberger

B.S. SUNY College of Environmental Science and Forestry

(1999)

Acknowledgements

My sincerest thanks go to the following:

Fumio Nakaya for financial support of this research

Dr. Ohta for his guidance and knowledge

Mitch Rosen, who provided the major ideas, concepts, and direction for this research, for having patience and confidence in me.

Lawrence Taplin, Garrett Johnson, and Anthony Calabria for patiently teaching me the ropes of programming

The faculty, staff, and students of the Munsell Color Science Laboratory

My parents and friends for backing every career decision I made

My brother Tim who unknowingly pushed me to do my best

And to my love Sara, who patiently supported me and motivated me through the best and the worst

This research was made possible by the generous financial support of

Fuji Xerox Corporation

TABLE OF CONTENTS

1	INTRODUCTION	1-1
1.1	<i>Scope of Research</i>	1-1
1.2	<i>Research Objectives</i>	1-4
2	SYSTEM CHARACTERIZATION	2-1
2.1	<i>Printer Characterization</i>	2-1
2.2	<i>Spectrophotometric Measurements</i>	2-5
2.3	<i>Printer Model</i>	2-6
3	CHARACTERIZATION EVALUATION	3-1
3.1	<i>System Precision Analysis</i>	3-1
3.2	<i>Determining Spectra For Unprintable Ink Combinations</i>	3-2
3.3	<i>Printer Model Accuracy</i>	3-5
4	INK VARIABILITY ANALYSIS ALGORITHM	4-1
4.1	<i>The Algorithm In Detail</i>	4-3
4.2	<i>Alternative Algorithms</i>	4-6
4.3	<i>Analyzing An Ink Variability Profile</i>	4-9
5	INK SPECTRAL INDEPENDENCE	5-1
6	MIDPOINT DATASET ANALYSIS	6-1
6.1	<i>Ink Variability Results</i>	6-1
6.2	<i>Ink Variability Density Maps</i>	6-7
6.3	<i>Colorimetric Evaluation Without The Black Ink</i>	6-14
7	LUT NODE ANALYSIS	7-1
7.1	<i>Ink Variability Results</i>	7-1
7.2	<i>Ink Variability Density Maps</i>	7-6
7.3	<i>Colorimetric Evaluation Without The Black Ink</i>	7-10
8	MIDPOINT AND LUT NODE CONCLUSIONS	8-1
9	SPECTRAL ERROR METRIC INVESTIGATION	9-1

10	THE INFLUENCE OF SPECTRAL REDUNDANCY ON SPECTRAL COLOR MANAGEMENT	10-1
10.1	<i>Spectral Color Management</i>	10-1
10.2	<i>The Influence of Spectrally Stable Ink Variability on Multi-Dimensional Lookup Tables</i>	10-3
10.3	<i>Experimental</i>	10-5
10.4	<i>Conclusions</i>	10-7
11	SPECTRALLY TRANSLUCENT WATERMARKING	11-1
11.1	<i>Level 1: Embedding Information In A Uniform Color Patch</i>	11-2
11.2	<i>Level 2: Simple Image Watermarking</i>	11-4
11.3	<i>Level 3: Complex Image Watermarking</i>	11-6
12	CONCLUSIONS	12-1
12.1	<i>Future Research</i>	12-2
REFERENCES		
APPENDIX A. MATLAB CODE		
A-1	<i>Printer Model</i>	A-2
A-2	<i>Spectrally stable Multi-ink Variability Algorithm</i>	A-2
A-3	<i>Code To Create Density Maps For The Midpoint Dataset</i>	A-4
A-4	<i>Code To Create Density Maps For The LUT Node Factorial Sampling</i>	A-6
A-5	<i>Level 1: Embedding Information In A Uniform Color Patch</i>	A-7
A-6	<i>Level 2: Simple Image Watermarking</i>	A-8
A-7	<i>Level 3: Complex Image Watermarking</i>	A-9
APPENDIX B. SPECTRALLY REDUNDANT MIDPOINT SAMPLES		
		B-1
APPENDIX C. SPECTRALLY REDUNDANT LUT NODE SAMPLES		
		C-1
APPENDIX D. SPECTRALLY REDUNDANT MIDPOINT SAMPLES USED IN SPECTRAL ERROR METRIC INVESTIGATION		
		D-1
APPENDIX E. SAMPLES EXHIBITING INTERPOLATION ERRORS BETWEEN NODES		
		E-1

APPENDIX F. SPECTRAL WATERMARKING EXAMPLES	F-1
<i>Level 1: Watermarked Image</i>	F-3
<i>Level 1: Ink Separations</i>	F-4
<i>Level 2: Watermarked Image</i>	F-5
<i>Level 2: Ink Separations</i>	F-6
<i>Level 3: Original Image (Left), Watermarked Image (Right)</i>	F-7
<i>Level 3: Cyan (Left) and Magenta (Right) Ink Separations</i>	F-8
<i>Level 3: Yellow (Left) and Black (Right) Ink Separations</i>	F-9
<i>Level 3: Green (Left) and Orange (Right) Ink Separations</i>	F-10

1 INTRODUCTION

1.1 *Scope of Research*

The development of six-ink printing systems has reached far beyond the limitations of four-ink printing.¹⁻¹⁰ Investigations on the capabilities of six-ink printing are far from exhausted. This research focuses on developing algorithms and methods to understand ink level variability tolerancing within spectral reproduction systems. The observation that many different ink combinations within a multi-ink inkjet printer can approximately produce the same spectral reflectance was first reported by Rosen *et al.*¹ and further investigated by Chen and co-workers at the Munsell Color Science Laboratory (MCSL). This investigation further quantifies the phenomenon through the development of techniques that systematically analyze ink sets to determine spectrally stable ink variability ranges. This also includes developing effective means of visualizing multidimensional data to illustrate the ink variability ranges throughout the six-dimensional ink space.

Spectrally stable ink level variability in a printing system is worth investigating because understanding this occurrence allows effective transforms to be built for spectral color management. The techniques can also be used to assist in the search for better spectral reproduction metrics. In addition, the analysis of spectral redundancy allows the degrees of spectral matching freedom within a printing system to be determined. This has a direct influence on ink selection for printing system fabrication, and ink design for spectral reproduction systems. This analysis also provides the potential for previously unconsidered applications not possible until now.

Spectrally stable ink level variability in a printing system is also referred to as spectral redundancy.¹¹ The concept of spectral redundancy can be compared to the theories of

colorimetric redundancy. In a colorimetric system, development of CMYK printing techniques such as gray component replacement (GCR) and under-color removal (UCR) maintain colorimetric accuracy by replacing some quantity of colored inks with black ink.¹² Colorimetric redundancy does not necessarily hold as viewing conditions or observers change because of metamerism. The advantage of spectral redundancy over colorimetric redundancy is that different ink combinations creating a spectral match within tolerance means that color match will hold for all observers across any viewing conditions.

One very important parameter to consider when evaluating spectrally stable ink variability in a printing system is the selection of a spectral difference metric to determine when a spectral match has been made. Due to sources of error in measurement and printing systems, two spectra are considered a match only when a tolerance range is specified. In addition to noise, two curves are also considered spectrally similar when they fall within the application specific tolerance range.

Evaluating spectral curve metrics is still an ongoing area of research.¹³ Current spectral difference metrics include RMS error, and Hernández-Andrés goodness of fit coefficient (GFC).¹⁴ Weighted RMS metrics have also been evaluated. They include inverse of the reflectance spectra and diagonal matrix $[\mathbf{R}]$.¹⁵ It is important to select a metric and tolerance range appropriate to a particular system being evaluated and its target application.

The procedures developed to analyze spectrally stable ink variability can be used in the evaluation of spectral difference metrics. Because the developed algorithms can use any spectral difference metric, the process can be used to evaluate and search for those best related to user experiences. The advantage lies in the ability to print and compare images visually so that spectral difference metrics can be evaluated.

This research also provides the ability to determine the degrees of spectral matching freedom within a printing system for a given spectral matching metric and a specified tolerance range. When the spectra of all ink combinations using a particular ink can be matched by ink combinations not using the particular ink at all, the degrees of freedom for matching spectra are reduced for the printer because the other inks cover the entire spectral gamut of the matched ink. The ability to determine this has a direct impact on ink design and specifying inks for system fabrication.

Inks that are linearly independent cannot be matched using any combination of the other inks. Depending on the application it may be advantageous to minimize spectral redundancy thus maximizing the spectral gamut of the printer. For other applications, it may be preferable to design printers that have numerous spectrally redundant ink combinations. This opens the door to new applications such as spectrally translucent watermarking.

System precision requirements could also be defined using the techniques developed from this study. It is possible to determine how much an ink can vary while still producing a spectral match within a specified tolerance range.

Finally, spectral color management is greatly influenced. Because of spectral redundancy in a system, a lookup table (LUT) relating spectra to printer digital counts can be spectrally consistent but inconsistent in ink space. This can create an interpolation disaster. By understanding the relationship between spectra and ink levels, processes can be developed to control both spaces to maximize interpolation stability.

1.2 Research Objectives

The efforts of this research are focused at the interface between image processing and spectral based printing. Figure 1-1 shows the concentration of this research with respect to the entire spectral image reproduction system.

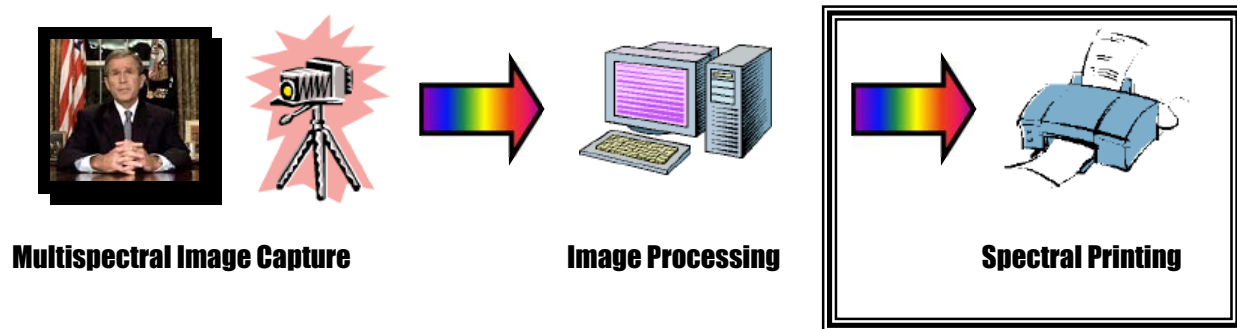


Figure 1-1. Diagram of an end-to-end spectral reproduction system. The outline area indicates the focus of these research efforts.

The process developed to conduct this research included several phases. The first phase involved spectral characterization of the printer to relate input printer digital counts to output printed spectra. Next, an algorithm systematically evaluated the ink variability for given spectral reflectance and was applied to a factorial sampling of ink space. Based on these results, a multidimensional mapping visualization showed the ink variability ranges throughout ink space. Finally, the results of the algorithm were used to explore the impact on multidimensional color management look up tables, and the potential for spectrally translucent watermarking.

2 SYSTEM CHARACTERIZATION

A platform was needed to implement the techniques developed for evaluating spectrally stable ink-level variability. A six-ink ink-jet printer was selected and spectrally characterized using a technique previously demonstrated by Rosen, et al.⁵ The printer was configured with cyan, magenta, yellow, black, green, and orange inks. The inks were not chosen by any criteria other than availability.

2.1 *Printer Characterization*

The six-ink printer shown in Figure 2-1 was characterized for this research. This printer was used at a resolution of 720 x 720 dpi. The printing medium was an A3 size (13 by 19 inch) MC design glossy paper DDK 0366.



Figure 2-1. CMYKGO printer.

Linearity between percent area coverage and printer digital counts was achieved for individual inks. Data for this analysis was obtained by printing two pages of five ramps per page for each ink. On the two pages, the ramps were spatially offset to account for spatial variation of the printer. The digital counts were converted to percent area coverage using a spline based lookup table. A complete five-way factorial sampling of all ink combinations was designed using this derived relationship. Patches representing all combinations of inks at 0%, 25%, 50%, 75%, and 100% area coverages were printed.

The complete six-ink factorial division of the ink space consisted of 5^6 or 15,625 samples. If each sample represents a vertex in the six-dimensional ink space, then a single hypercube is built from 64 contiguous vertices. The center point of each hypercube is called a midpoint. A midpoint is equidistant from every vertex that comprises its surrounding hypercube. On each page of the characterization patches, 256 of the 4^6 or 4,096 midpoints of this factorial design were included. The midpoints were described by the factorial design of the percent area coverages of 12.5%, 37.5%, 62.5%, and 87.5%.

A set of twelve different patches at each corner and twenty various patches at the center of the page were included for quality control purposes. In addition, individual color ramps were printed on the first and last page. Each page contained 1,320 5/16-inch square patches in 44 rows and 30 columns. In total, 16 pages totaling 21,120 patches were printed. Diagnostic prints were made before and after each page to verify that the printer jets were not clogged. The digital counts used for the five-way factorial and the midpoints are shown in Table 2-1 and 2-2 respectively.

Table 2-1. Digital counts used in the 5⁶ factorial sampling of ink space.

Area Coverage	Cyan	Magenta	Yellow	Black	Green	Orange
0%	0	0	0	0	0	0
25%	15	13	23	6	20	12
50%	40	36	63	16	55	32
75%	92	84	133	33	120	78
100%	255	255	253	233	255	255

Table 2-2. Digital counts used in the 4⁶ midpoint factorial sampling of ink space.

Area Coverage	Cyan	Magenta	Yellow	Black	Green	Orange
12.5%	7	6	11	3	9	5
37.5%	26	22	39	11	35	21
62.5%	61	56	93	23	83	51
87.5%	144	131	186	54	173	126

Note that digital count values of 233 for the black channel and 253 for the yellow channel were selected because full dot coverage was obtained at these values. The lookup tables are shown in Figure 2-2.

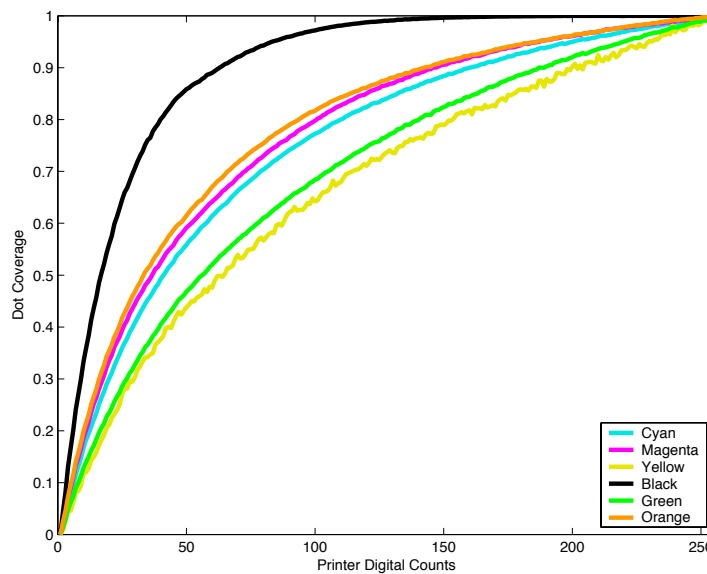


Figure 2-2. One-dimensional lookup tables used to determine the relationship between printer digital counts and area coverage.

The lookup table developed for the yellow channel in Figure 2-2 was much more uneven than the other five inks in the system. To examine why the yellow curve appeared to be more noisy, digital counts versus luminance factor were plotted for all six inks of the printer. This is shown in Figure 2-3. In this plot, all the inks have similar magnitudes of variability.

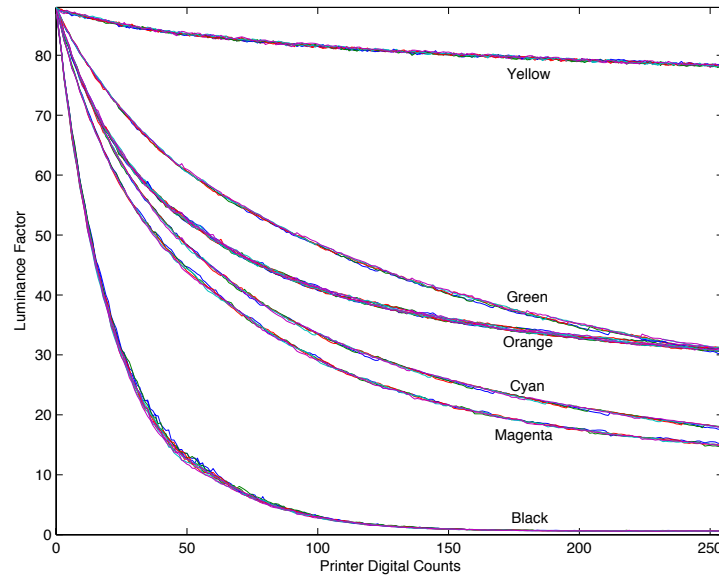


Figure 2-3. Relationship between printer digital counts and luminance factor for the six channels of the printer.

The curves shown in Figure 2-2 are based on the relationship between area coverage and digital counts. As shown in Figure 2-3, the luminance factor range of the yellow ink is much smaller than the other inks. Luminance factor was used to calculate area coverage thus the apparent noise is magnified when normalizing the curves. The variations seen in Figure 2-2 are consequently a result of scaling differences for each channel.

2.2 Spectrophotometric Measurements

A GretagMacbeth Spectrolino Spectroscan illustrated in Figure 2-4 was used to obtain all spectral measurements for this research. Mounted to a transverse and longitudinal positioning table, the spectrophotometer has 45°/0° bi-directional illumination/viewing geometry with a 4mm diameter aperture.

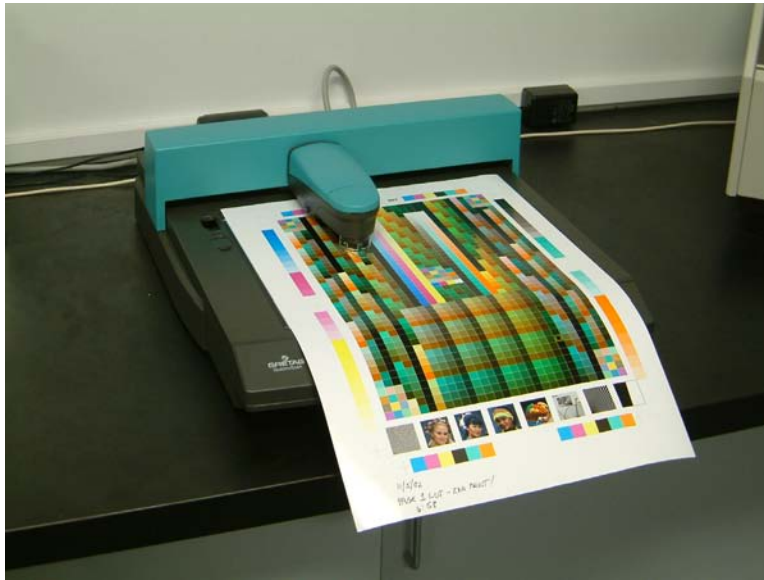


Figure 2-4. Gretag Macbeth Spectrolino Spectroscan spectrophotometer.

The reflectance of each patch was sampled from 380nm to 730nm at 10nm intervals. Each page was allowed to dry a minimum of 4 hours before being measured. Because the paper size was larger than the maximum longitudinal and transversal movement of 9.4 inches and 12.2 inches respectively, the upper half of the page was measured first and then the page was moved to measure the lower half.

2.3 Printer Model

The forward printer model was constructed using the five-way factorial sampling of all digital count combinations shown in Table 2-1 and the associated measured spectral reflectances. A six-dimensional LUT was built relating the input of percent area coverage to printed spectra. Based on the input six-ink area coverage combination, six-dimensional linear interpolation was used to predict the printed spectral reflectance. To convert from digital counts to spectra, a set of six one-dimensional LUTs (shown in Figure 2-2) preceded application of the six-dimensional LUT. The MATLAB code for the forward printer model is located in Appendix A (A-1). The evaluation of this printer model is discussed in Chapter 3.

3 CHARACTERIZATION EVALUATION

3.1 System Precision Analysis

An experiment was conducted to determine the source of noise in our system. Included in this test were inter-instrument measurement variability, variation across our print medium, and printer variation across a page. The average and maximum root-mean-squared (RMS) error between measurements for a given patch were used as the evaluation metrics.

The characterization pages described in the previous chapter were evaluated. On one page, the upper left, upper right, and corresponding central quality control patches were measured three times without replacement, and three times with replacement. The upper left group of quality control patches was defined as the standard and referred to as Control Target 1. Without replacement was defined as measuring the upper half of the page (22 rows and 30 columns) three times in a row without moving the paper. With replacement data was collected similarly except that the page was removed and realigned between each of the three measurements. Each of the three measurements was defined as Measurement 1, Measurement 2, and Measurement 3. With the 12 upper right quality control patches of the first measurement defined as the standard, comparisons made between the upper left (Control Target 2) and central quality control patches (Control Target 3) for each measurement are shown in Table 3-1.

Table 3-1. Mean and maximum RMS error between the upper left standard target (std.) and the upper right and center targets of page 1.

Without Replacement						
	Measurement 1		Measurement 2		Measurement 3	
	Mean	Max	Mean	Max	Mean	Max
Control Target 1	Std.	Std.	0.0019	0.0030	0.0024	0.0039
Control Target 2	0.0046	0.0061	0.0047	0.0062	0.0047	0.0063
Control Target 3	0.0038	0.0098	0.0042	0.0099	0.0044	0.0103
With Replacement						
	Measurement 1		Measurement 2		Measurement 3	
	Mean	Max	Mean	Max	Mean	Max
Control Target 1	0.0024	0.0039	0.0019	0.0031	0.0025	0.0039
Control Target 2	0.0047	0.0063	0.0047	0.0067	0.0046	0.0064
Control Target 3	0.0044	0.0103	0.0043	0.0100	0.0045	0.0099

The smallest mean and maximum RMS errors were for measurements 1, 2, and 3 of control target one without and with replacement. Because the same control target was evaluated, this can be viewed as the precision of the instrument. Previous testing of the instrument within the MCSL has shown similar RMS error results when measuring BCRA Tiles over various time frames.

The largest mean and maximum RMS errors of 0.0044 and 0.0103 respectively were found when comparing the standard target to Control Target 3 with replacement. These measurements included inter-instrument variability, paper variation, and printer variation.

3.2 Determining Spectra For Unprintable Ink Combinations

The largest problem encountered when printing the 5⁶ LUT node points and 4⁶ midpoints as described in Tables 2-1 and 2-2 respectively was ink pooling for some ink combinations totaling greater than 200% area coverage. Pooling was when ink puddled on the surface of the paper because it was not fully absorbed. This was a result of printing on a coated medium with

relatively low ink absorption. An exhaustive analysis of the 19,721 printed patches was conducted by visually inspecting every patch. A patch was rated at one of three levels: OK, scroll or blot. Examples of scrolled and blotted patches are shown in Figure 3-1. All ink combinations that yielded scrolled or blotted patches were considered unprintable.

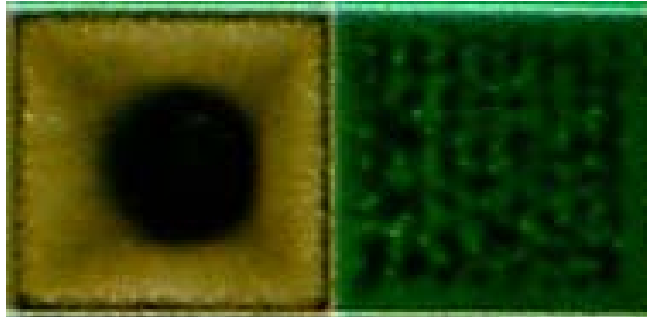


Figure 3-1. Printed color patches exhibiting blotting (left) and scrolling (right).

Current research within the MCSL has developed a model to statistically predict the spectral reflectance of six-ink percent area coverage combinations outside the printable range. Having this unprintable ink combination model at our disposal, the measured spectra of the blotted and scrolled six-ink combinations were compared to those predicted by the model. The measured reflectance for a blotted or scrolled color patch was determined by averaging the spectral reflectance over a 4 mm diameter aperture area. Out of 19,721 LUT nodes and midpoints printed, approximately 11.8% exhibited scrolling and 15.5% exhibited blotting.

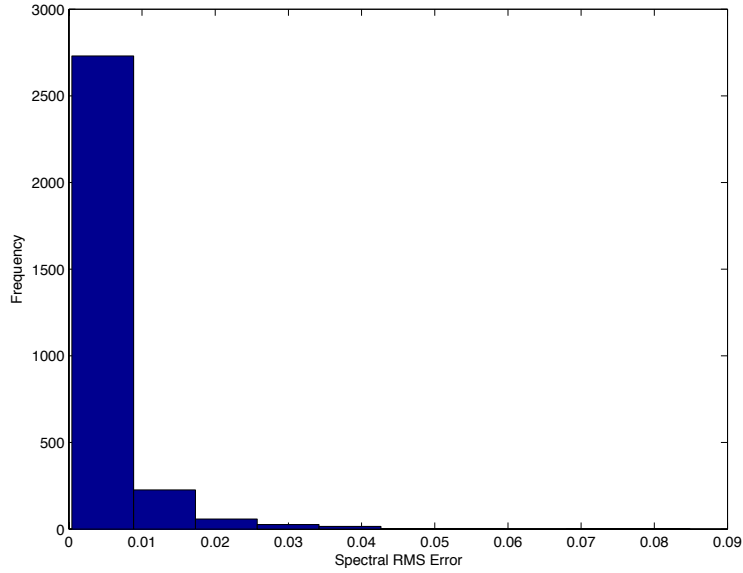


Figure 3-2. RMS histogram of the difference between the interpolated and measured spectral reflectances for the scrolled patches.

Figure 3-2 shows a histogram of RMS error between the measured spectral reflectances and the model predicted spectral reflectances for the scrolled ink patches. The average RMS error was 0.005 with a maximum of 0.085.

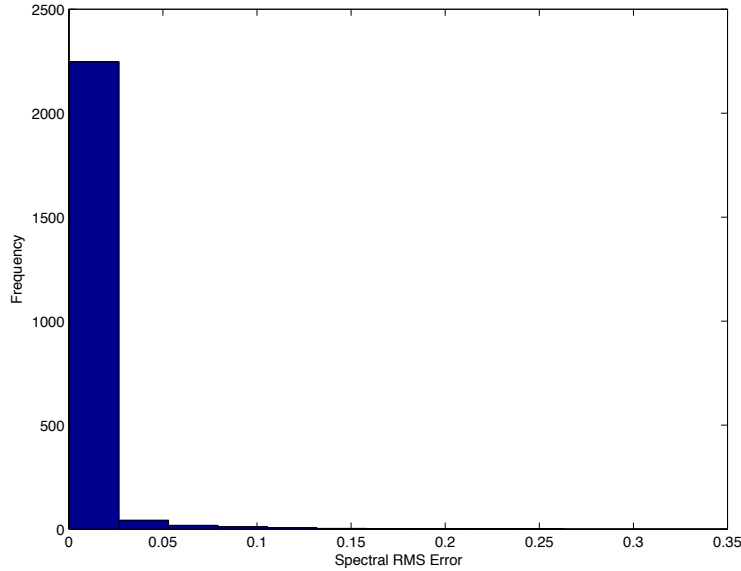


Figure 3-3. RMS histogram of the difference between the interpolated and measured spectral reflectances for the blotted patches.

A histogram of RMS error is also shown in Figure 3-3 for the measured spectral reflectances compared to the model predicted spectral reflectances for the blotted ink patches. The average RMS error was 0.009 with a maximum of 0.263. One reason for the large maximum RMS error for the blotted patches is due to contamination from neighboring pooled patches that occurred during the printing process.

To determine the spectral reflectances to be substituted by the unprintable ink combination model, a tolerance of 0.009 spectral RMS error (roughly equal to the combined maximum precision variability of the printer, paper, and instrument) was chosen.

3.3 Printer Model Accuracy

The accuracy of the forward printer model relating percent area coverage to spectral reflectance was evaluated by comparing measured spectral reflectance of the printable midpoints to the LUT

interpolated spectral reflectance. It was determined that out of the 4,096 midpoint dataset, 3,889 did not create blotted or scrolled patches (as shown in Figure 3-1) and were considered printable.

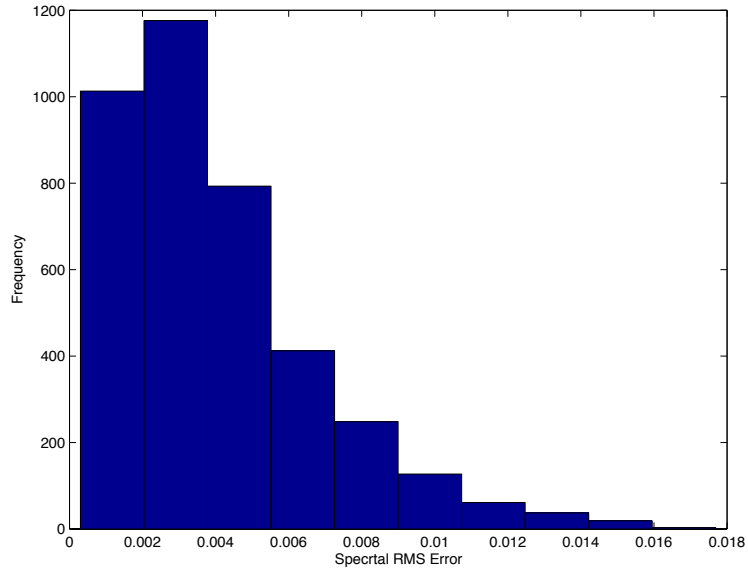


Figure 3-4. RMS histogram of the difference between the interpolated and measured spectral reflectances of the 4,096 midpoints.

Figure 3-4 shows a histogram of RMS error when comparing the interpolated spectrum to the measured spectrum. The average RMS error was 0.004 with a maximum of 0.017. Color differences in ΔE_{00} units were also calculated between the interpolated and measured spectral reflectances using illuminant D65 and the 1931 standard 2-degree observer.

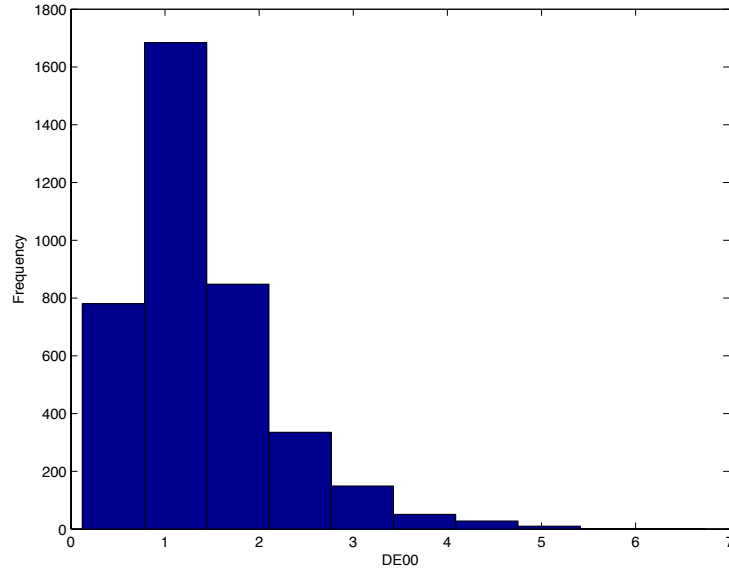


Figure 3-5. ΔE_{00} histogram of the difference between the interpolated and measured spectral reflectance of the 4,096 midpoints.

A histogram showing the color differences is shown in Figure 3-5. The average and maximum ΔE_{00} were 1.5 and 6.7 respectively. The error in the printer model can be attributed to many factors. They include spectral reflectance measurement errors in the midpoint and LUT characterization datasets, interpolation error, and spectral reflectance prediction errors based on the unprintable ink combination model.

4 INK VARIABILITY ANALYSIS ALGORITHM

To evaluate spectrally stable ink variability in a printer, it was necessary to devise a procedure that would systematically determine throughout ink space how much individual inks could be changed while introducing as little spectral error as possible. The concept of maintaining spectra relies on the choice of spectral difference evaluation metrics and tolerances chosen for specific needs. The algorithm employs an evaluation metric during analysis but the technique does not rely on any specific metric. Reanalysis of the same printer may be based on different evaluation metrics. Tolerances can be chosen after analysis and may be changed without need of reapplying the algorithm.

The analysis protocol required a model that could predict printed reflectance spectra from ink fractional area coverages. Such a model for our printer was developed in Chapter 2. Many digital count combinations were analyzed throughout the printer's ink gamut to establish the amount of spectral redundancy for an ink at a particular area in the gamut. Figure 4-1 illustrates the procedure used to uncover spectrally stable ink variability.

The digital counts were related to ink fractional area coverages by one-dimensional LUTs. For each digital count combination, the reflectance spectrum was derived through the forward model. Each ink plane was separately analyzed using a routine that manipulated the ink digital count from one plane by a single value for each pass. An iterative model inversion optimized the other five ink digital counts to match the original reflectance spectrum as close as possible given the manipulated ink digital count. The resultant digital counts and the spectral difference between the predicted reflectance and that of the original were reported. This procedure was repeated at each digital count in all the ink planes for a sample.

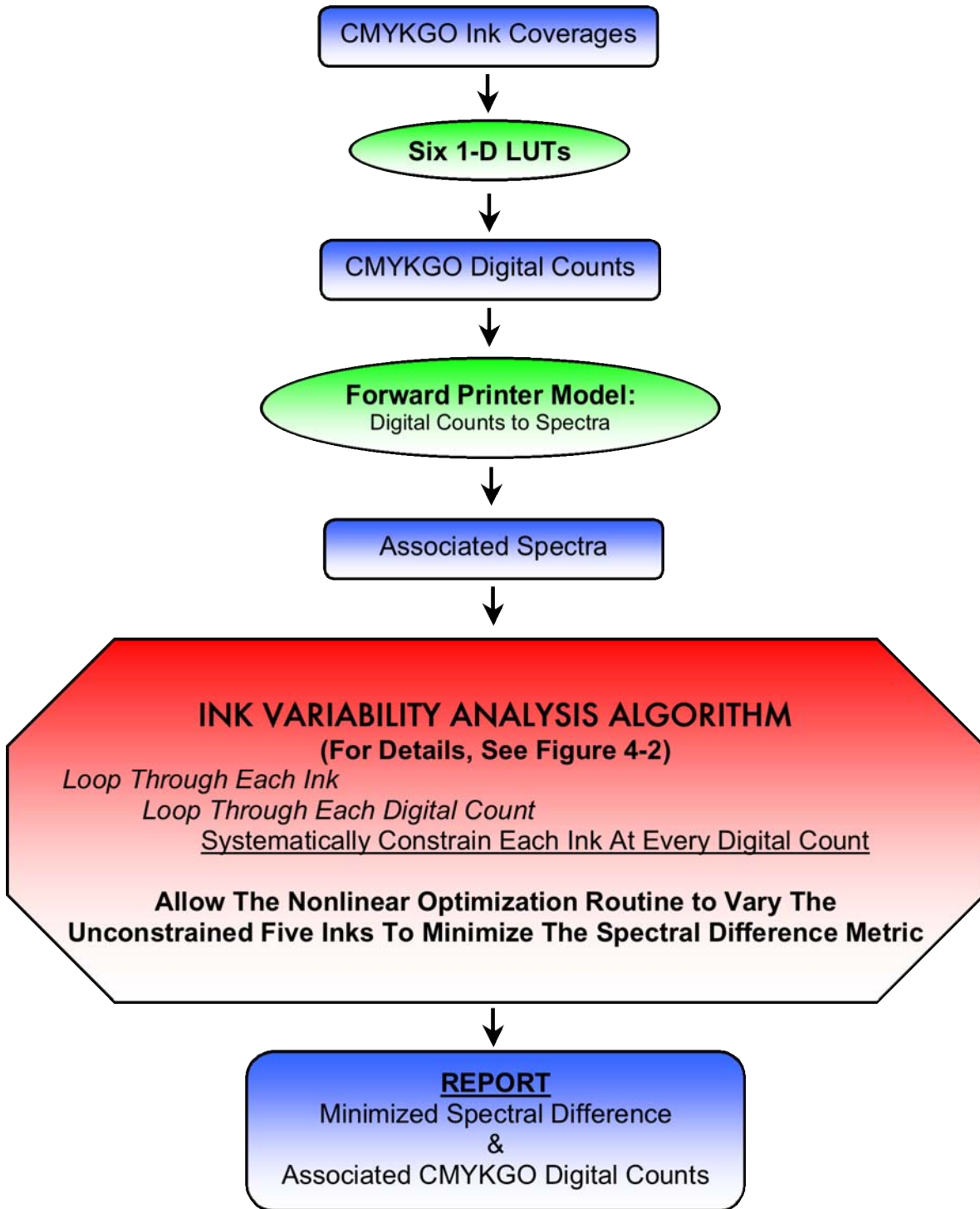


Figure 4-1. General outline of spectrally stable multi-ink variability algorithm.

The optimization routine *fmincon* found in the MATLAB optimization toolbox was used to invert the forward printer model. These types of routines are usually susceptible to local minima; however, the algorithm employed in this study was particularly robust to that problem. The initial starting values were obtained from the original digital count combination that was used to predict the spectral reflectance in the printer model. At each iteration, the digital count value for one ink was modified by a single digital count, thus the seeded starting value was a very good first approximation.

4.1 The Algorithm in Detail

The algorithm developed to determine the spectrally stable ink variability used CMYKGO digital counts as the initial input. The CMYKGO percent area coverages were derived through six one-dimensional LUTs. The forward model was then used to interpolate the associated spectral reflectance for the initial six-ink combination. Using these parameters, the algorithm computed the range of ink variability for each ink that minimized the difference between the original and optimized spectra. For this experiment, spectral RMS was used as the metric to minimize. Other implementations could easily replace RMS with any error metric of interest.

Shown in Figure 4-2, the algorithm first selected one ink and systematically incremented by one digital count from its previous value. The incremented ink was considered the constrained ink. The optimization routine varied the other five inks to make the best spectral match possible while keeping the percent area coverages of the unconstrained inks between 0 and 100%. The six-ink combination (including the constrained ink) that produced the smallest RMS error was returned from the routine. This process was repeated until the ink was constrained from its initial digital count value to 255 digital counts. If the initial digital count

value of an ink was greater than zero digital counts, the algorithm returned to the initial values and systematically decremented by one digital count from its previous value. This was repeated until the ink was constrained from its initial digital count value to 0 digital counts. Because the best spectral match for this system occurred at the initial CMYKGO digital count combination, the starting values for each inversion were seeded with the values obtained from the previous inversion. This assisted the routine in avoiding local minima. The MATLAB source code for this algorithm is shown in Appendix A (A-2).

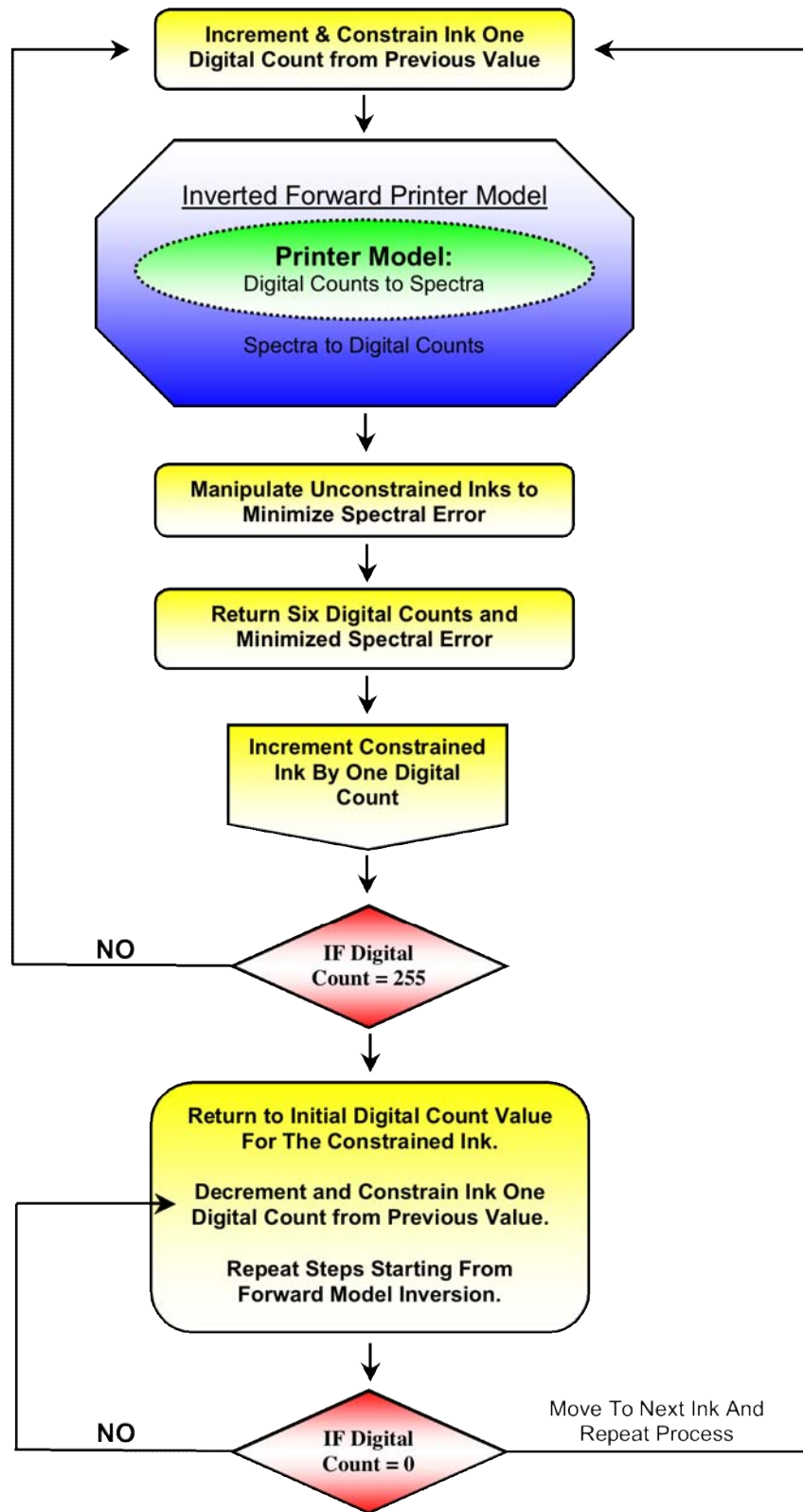


Figure 4-2. Algorithm developed for uncovering spectrally stable ink level variability.

A portion of the results from the analysis of a single spectrum using the algorithm is shown in Table 4-1 when yellow was the constrained ink. The original CMYKGO digital counts appear in bold red italics. The smallest RMS error was found at a yellow digital count of 39 because the starting point of the algorithm was always the initial CMYKGO ink combination.

Table 4-1. Results of the spectrally stable multi-ink variability algorithm when yellow was the constrained ink.

Constrained Digital Count (Yellow)	RMS Error	Cyan Digital Count	Magenta Digital Count	Black Digital Count	Green Digital Count	Orange Digital Count
34	0.0039	19	6	3	105	5
35	0.0038	20	6	3	103	5
36	0.0032	20	6	3	103	5
37	0.0030	20	6	3	102	5
38	0.0016	22	6	2	100	5
<i>39</i>	<i>0.0015</i>	<i>22</i>	<i>6</i>	<i>2</i>	<i>99</i>	<i>5</i>
40	0.0018	24	6	2	98	6
41	0.0018	24	7	2	97	6
42	0.0030	25	7	2	95	6
43	0.0033	27	7	1	94	6
44	0.0030	27	7	1	94	6

As the yellow ink was constrained further away from the initial digital count value, the algorithm had an increasingly difficult time minimizing the spectral difference. The initial RMS error was not zero for this particular example because the measured spectral reflectance was used as the input spectrum and the printer model was susceptible to interpolation error.

4.2 Alternative Algorithms

The algorithm approach selected for this research produced specific results. The method can be thought of as determining the sensitivity to varying ink levels for matching spectra throughout a printer's spectral gamut. For example, when a large range of ink levels can be used to match a

spectrum within a specified tolerance range in one area of a printer's spectral gamut for a particular ink, the system is less sensitive to changes in that ink at that particular spectral region of the printer gamut. When the range of ink levels for a specified tolerance is more limited, the ink level sensitivity is greater.

The technique used was not designed to specifically locate the greatest changes in ink levels for matching spectra. An alternative algorithm could use each of the characterization LUT nodes and midpoint six-ink combinations as starting points. This would allow for largely different ink combinations to be found, but would be very time consuming.

To refine such a modified method and make it more computationally feasible, only those six-ink combinations that produce similar spectra to the input spectral reflectance could be used as starting values. This would drastically reduce the number of computations. The results from this experiment may give several alternative answers depending on the frequency of six ink combinations that produced similar spectra. Because seeding occurs throughout the ink gamut, answers very different from the algorithm implemented in Figure 4-1 could result. A flow chart of this modified process is shown in Figure 4-3.

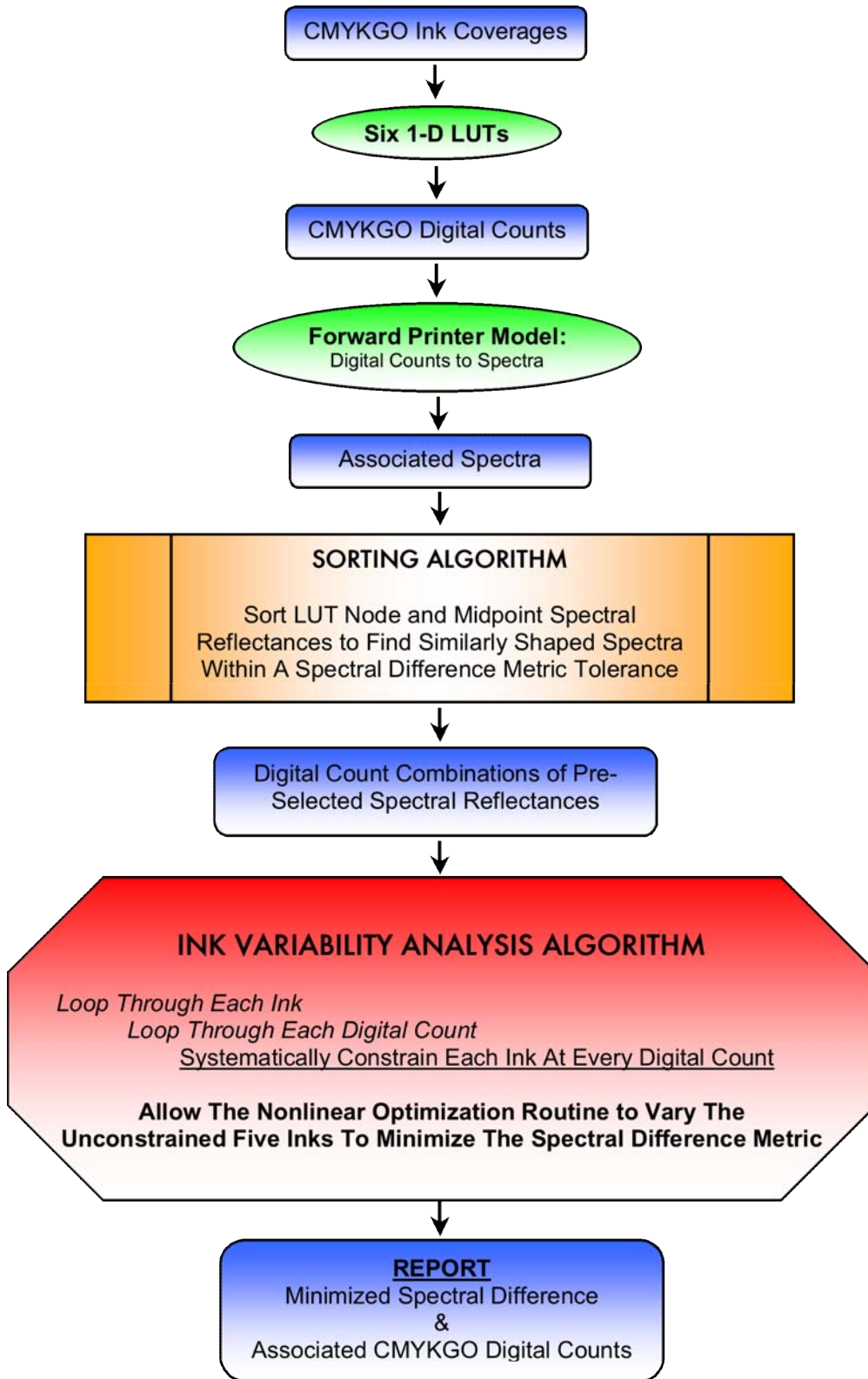


Figure 4-3. Flowchart of a modified algorithm that can determine largely different six-ink combinations.

4.3 Analyzing An Ink Variability Profile

A spectral match ink variability profile obtained from the algorithm explained in section 4.1 produces a variability profile for the spectrum originally printed CMYKGO ink combination of C=26, M=22, Y=11, K=11, G=35, O=126 as shown in Figure 4-4.

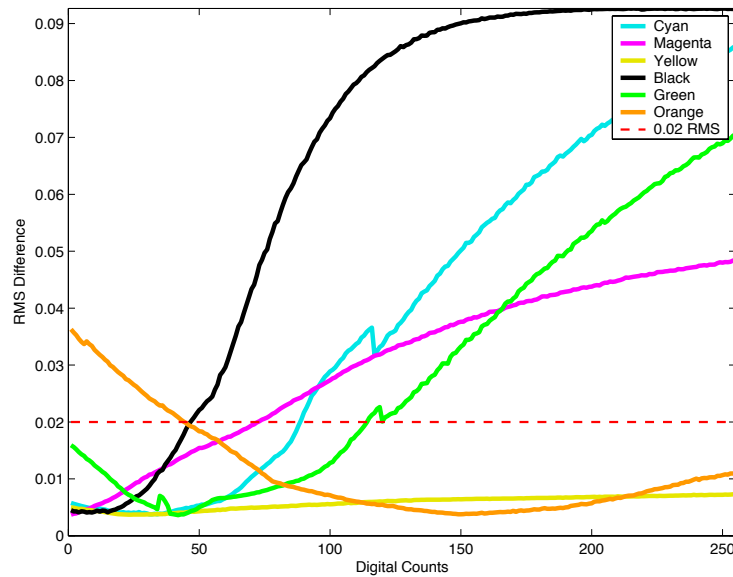


Figure 4-4. Spectral match ink variability profile for the spectrum printed by the digital count combination of C=26, M=22, Y=11, K=11, G=35, O=126.

Reviewing the spectral RMS error returned from the algorithm when the green ink was constrained, a kink in the curve can be seen around 125 digital counts. It was possible that this could be contributed to noise in the system; however it occurs at the 0.02 RMS tolerance level which is twice the within-sheet repeatability error. The same type of kink was also found in the cyan curve at approximately 125 digital counts. The kinks found in the cyan and green curves suggest that the algorithm attempted to converge at a very different digital count combination since the starting green value associated with this particular spectra was only 6 digital counts. It

is possible that a more sophisticated algorithm would be able to converge at a different location in spectral space.

5 INK SPECTRAL INDEPENDENCE

To determine if the individual ink reflectance spectra were linearly dependent, each ink at four concentrations was matched using the other five inks. This procedure was used for all six inks at 25%, 50%, 75% and 100% area coverages. Results for the ramps are shown in Figures 5-1 through 5-6.

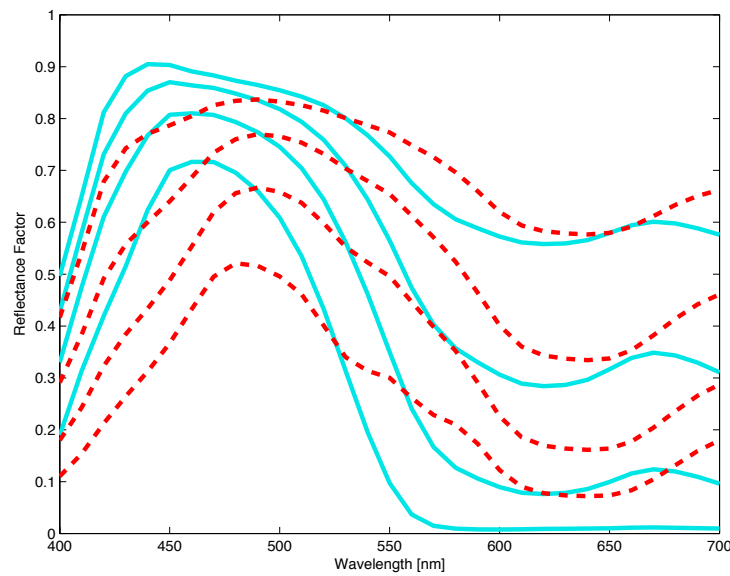


Figure 5-1. Cyan spectral independence. The solid lines are the cyan ramps and the broken lines are the estimated matches using the other five inks.

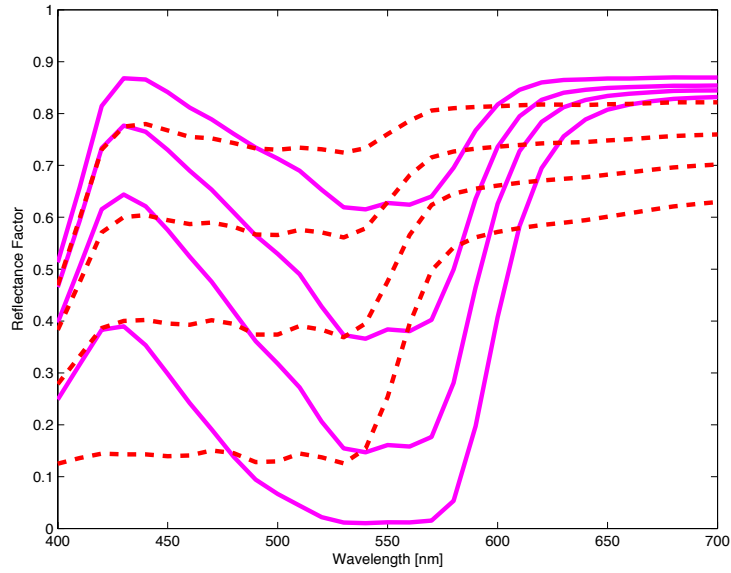


Figure 5-2. Magenta spectral independence. The solid lines are the magenta ramps and the broken lines are the estimated matches using the other five inks.

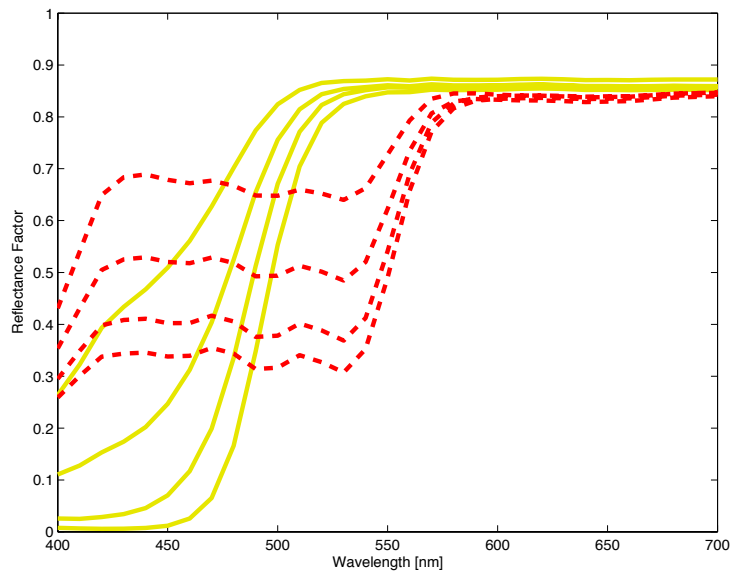


Figure 5-3. Yellow spectral independence. The solid lines are the yellow ramps and the broken lines are the estimated matches using the other five inks.

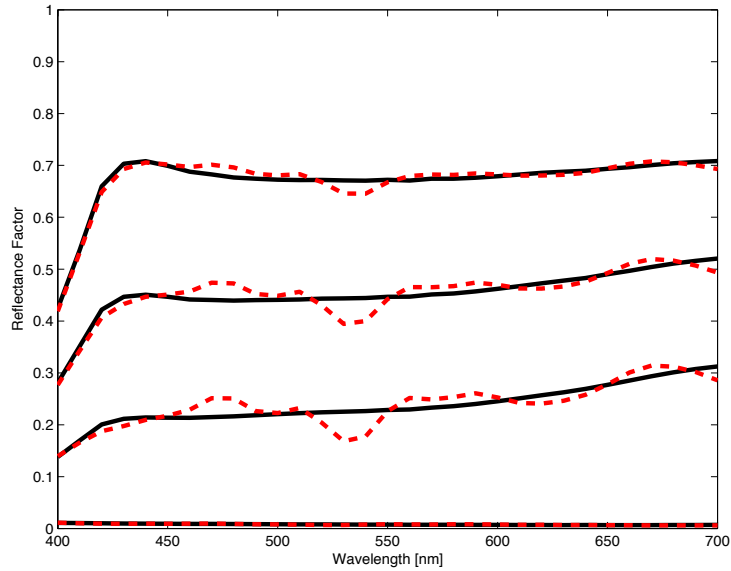


Figure 5-4. Black spectral independence. The solid lines are the black ramps and the broken lines are the estimated matches using the other five inks.

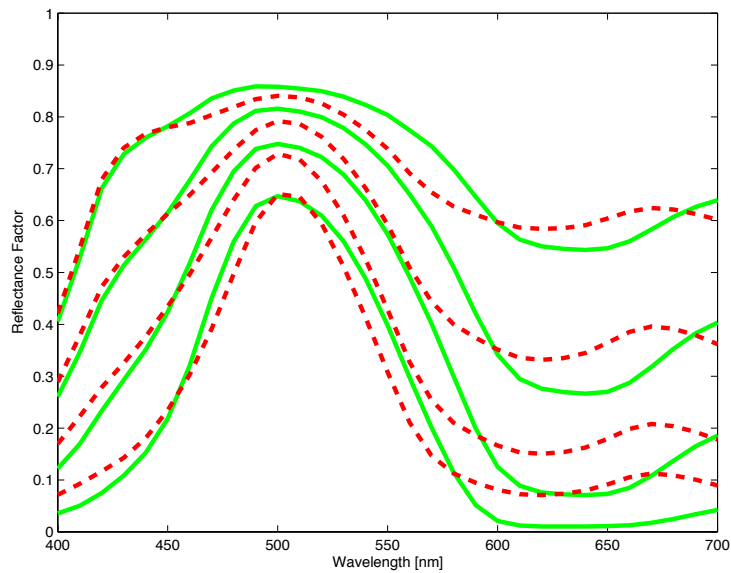


Figure 5-5. Green spectral independence. The solid lines are the green ramps and the broken lines are the estimated matches using the other five inks.

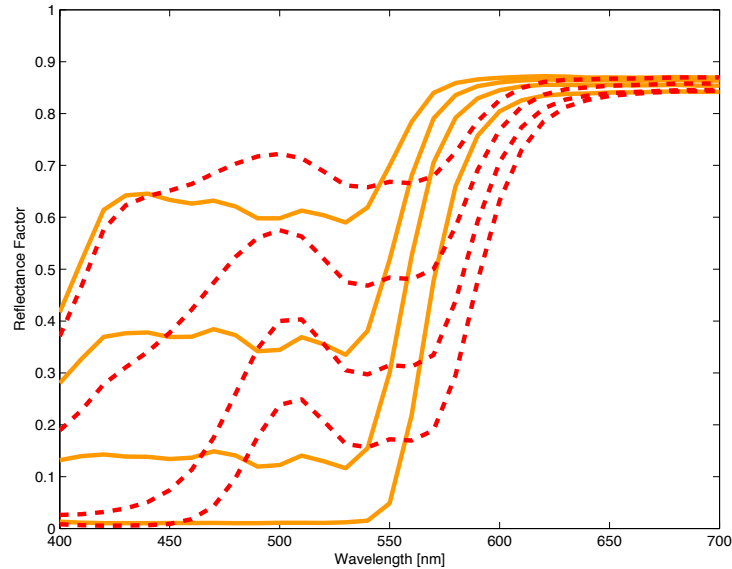


Figure 5-6. Orange spectral independence. The solid lines are the orange ramps and the broken lines are the estimated matches using the other five inks.

The RMS differences between the ramp spectra and the estimated spectra from the nonlinear optimization algorithm are shown in Table 5-1.

Table 5-1. RMS differences for Figure 5-1 through Figure 5-6.

Area Coverage	Cyan Ramp	Magenta Ramp	Yellow Ramp	Black Ramp	Green Ramp	Orange Ramp
25%	0.069	0.076	0.135	0.011	0.040	0.067
50%	0.131	0.144	0.203	0.019	0.066	0.125
75%	0.176	0.200	0.242	0.020	0.077	0.158
100%	0.167	0.218	0.247	0.001	0.057	0.137

The results show that the system had difficulty matching the ramp spectra for the chromatic inks. The minimum RMS difference of 0.04 RMS was found for the green ramp at 25% fractional area coverage and the maximum difference of 0.25 RMS for the yellow ramp at 100% area coverage.

The results for the black ink produced very interesting results. The largest RMS difference was 0.02; it was found for the black ink at a fractional area coverage of 75%. At the

smallest and largest fractional area coverages, the RMS difference was approximately equal to the within sheet variability of the system. If twice the within sheet variability or 0.02 RMS were selected as the spectral matching tolerance, the black ink in this system would be linearly dependent on the chromatic inks.

6 MIDPOINT DATASET ANALYSIS

6.1 *Ink Variability Results*

The algorithm developed to determine spectrally stable ink variability was applied to all 4,096 midpoint printed spectra. Ink variability density maps were built to indicate how the range of spectrally stable variability manifests throughout colorant space. A spectral reflectance factor RMS of 0.02 was chosen as tolerance since it was twice the system measurement and repeatability limit. Visualizations of ink variability density maps were complex because six-dimensional data was reduced to three dimensions for display.

At each node in the midpoint dataset the algorithm returned a spectral match ink variability profile as discussed in section 4.3. An example is shown in Figure 6-1 for the original six-ink digital count combination of C=7, M=6, Y=39, K=3, G=173, O=5. In the figure, each curve is associated with one of the six inks. The curves show the best spectral RMS error achieved by the algorithm when an ink was constrained at the digital count value shown on the ordinate axis. The dashed red line indicates where a 0.02 spectral RMS difference is reached.

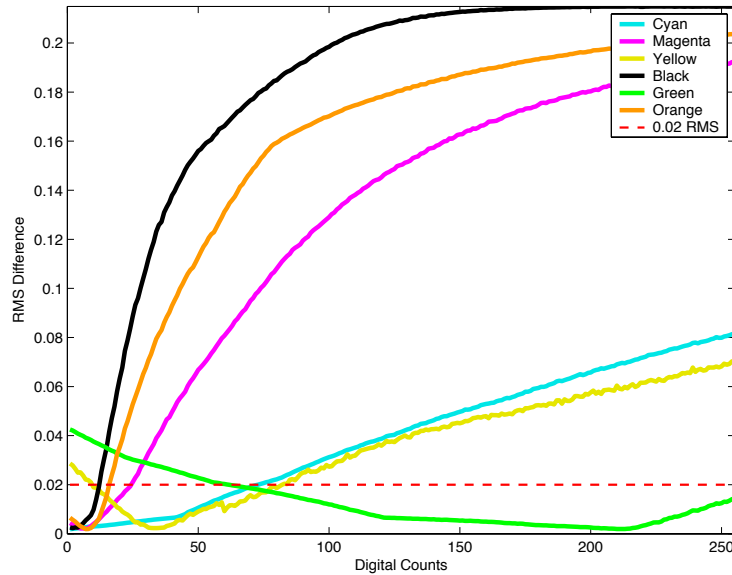


Figure 6-1. Example spectral match ink variability profile plot for the original printed spectra shown in Figure 6-2. The original six-ink digital combination was C=7, M=6, Y=39, K=3, G=173, O=5.

When 0.02 RMS is chosen as the tolerance limit, the portion of the curve that falls below that level shows the digital count range for the curve's associated ink that can maintain the original spectrum. The minimum RMS difference is approximately found where the ordinate digital count is equal to the original digital count. Interpolation errors in the characterization LUT and inversion routine precision limits cause the minimum values to vary slightly along the ordinate axis.

The original midpoint node spectral reflectance for Figure 6-1 contained 5 digital counts of orange. This is approximately where the minimum of the orange curve is located. As orange was systematically incremented, the system varied the other five inks to compensate so that the smallest spectral RMS difference was achieved. When orange was constrained at a digital count of 255, the smallest RMS difference was approximately 0.21. As the digital counts for an ink were constrained further away from the original value the RMS value generally increased.

Spectral match ink variability profile plots are shown on the left of Figures 6-2 through 6-7 for a selection of original spectra with luminance factors greater than or equal to 25. The right of each figure shows three spectra. The blue curve is associated with the measured spectral reflectance of the original midpoint CMYKGO digital counts. The black curve shows the maximum redundant spectrum. The maximum redundant spectrum results from the digital counts associated with the largest change in the indicated ink that maintains the original spectrum within a 0.02 RMS spectral difference factor. The red curve is the measured spectral reflectance of the maximum redundant printed CMYKGO digital counts. The printed samples discussed in Figures 6-2 through 6-7 are in Appendix B.

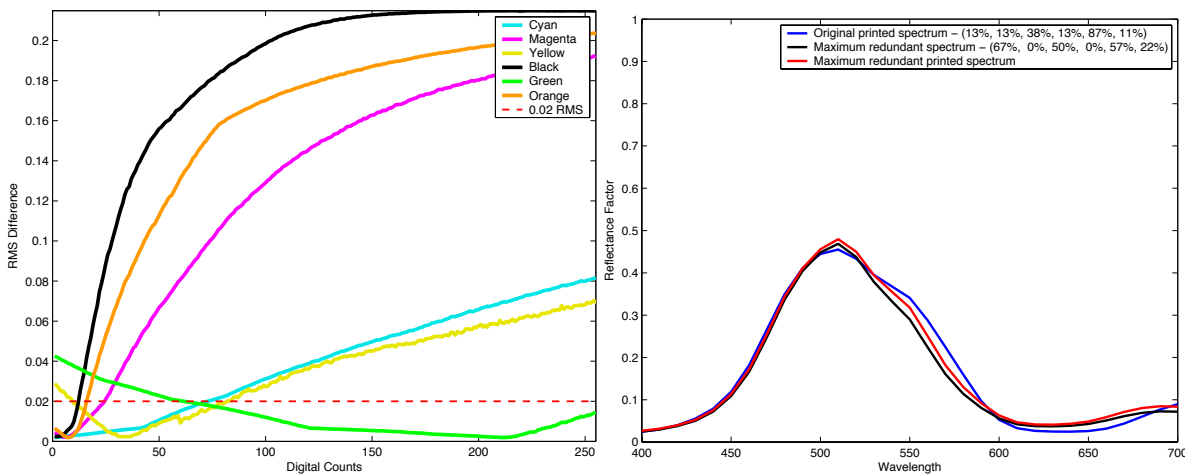


Figure 6-2. (Left) Spectral match ink variability profile for midpoint 77. (Right) Original, maximum redundant, and maximum redundant printed spectra. For the redundant spectra, cyan was increased 54% area coverage. See Appendix B sample MR-1a (original) and MR-1b (spectrally redundant printed).

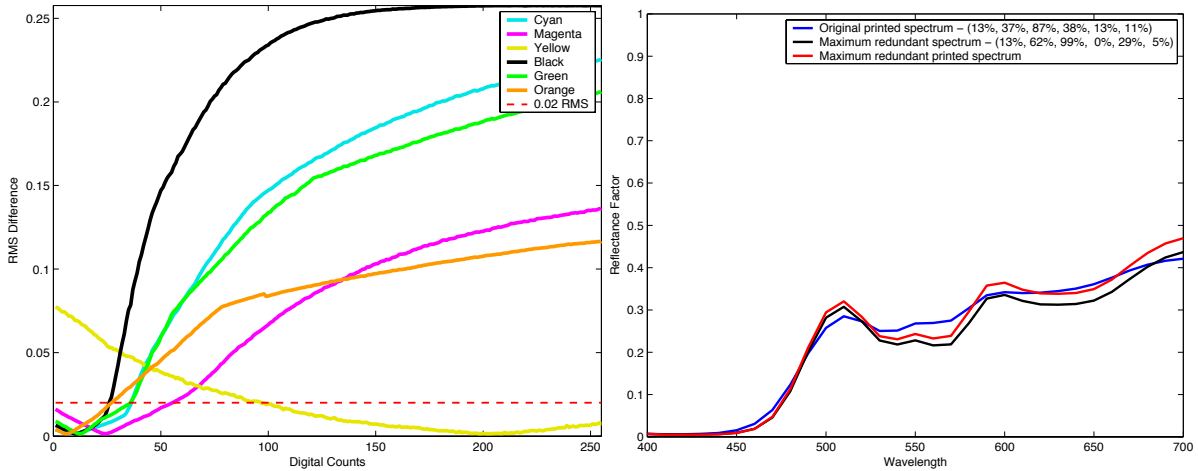


Figure 6-3. (Left) Spectral match ink variability profile for midpoint 465. (Right) Original, maximum redundant, and maximum redundant printed spectra. For the redundant spectra, magenta was increased 25% area coverage. See Appendix B sample MR-2a (original) and MR-2b (spectrally redundant printed).

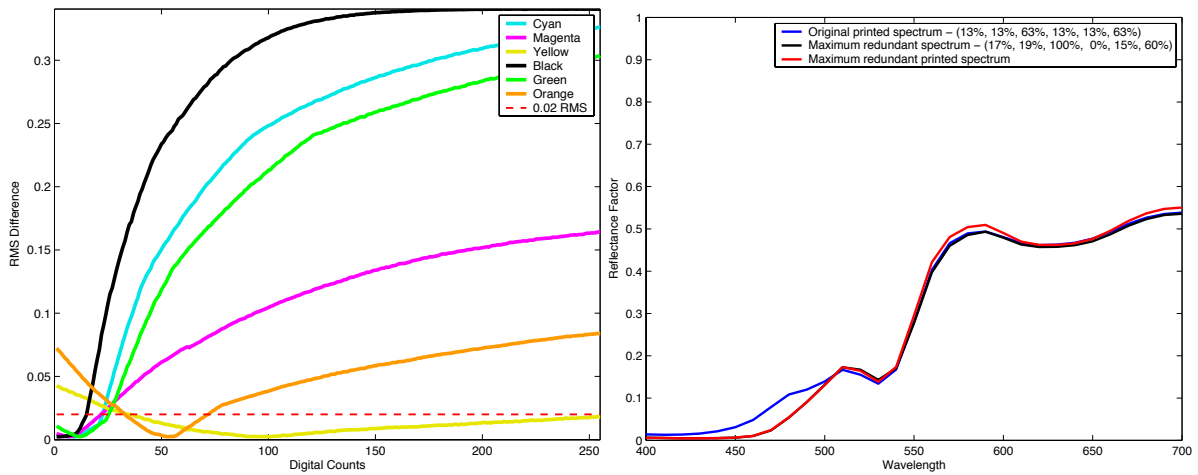


Figure 6-4. (Left) Spectral match ink variability profile for midpoint 131. (Right) Original, maximum redundant, and maximum redundant printed spectra. For the redundant spectra, yellow was increased 37% area coverage. See Appendix B sample MR-3a (original) and MR-3b (spectrally redundant printed).

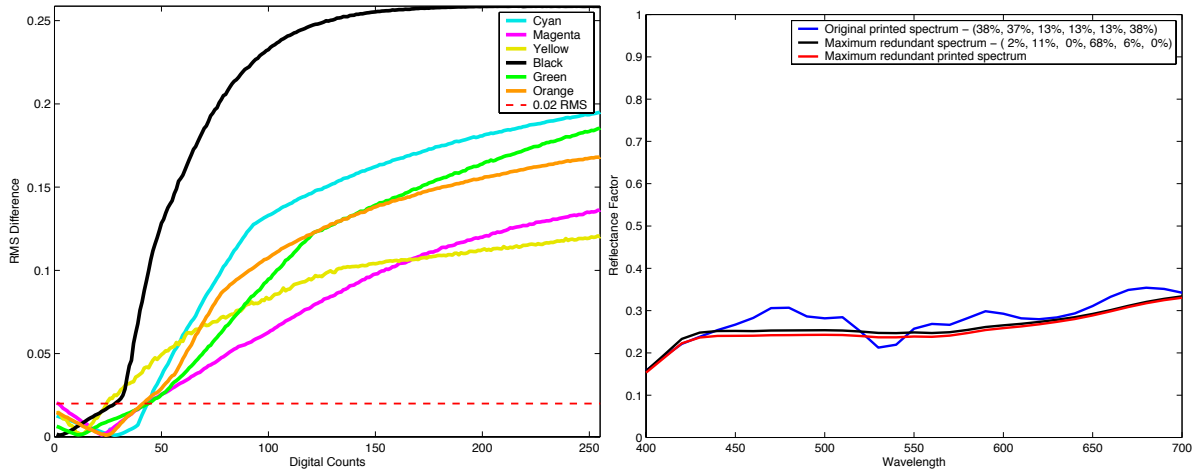


Figure 6-5. (Left) Spectral match ink variability profile for midpoint 1282. (Right) Original, maximum redundant, and maximum redundant printed spectra. For the redundant spectra, black was increased 55% area coverage. See Appendix B sample MR-4a (original) and MR-4b (spectrally redundant printed).

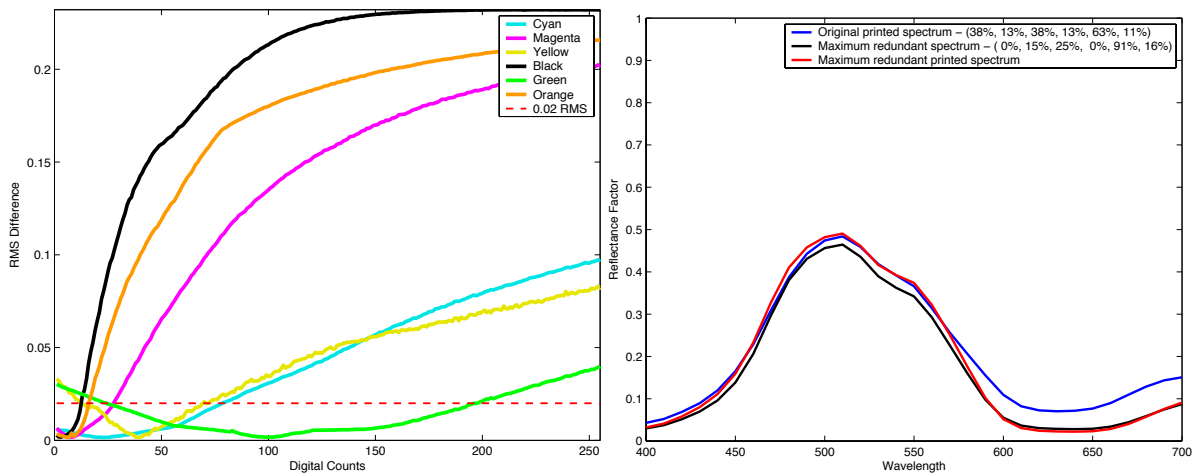


Figure 6-6. (Left) Spectral match ink variability profile for midpoint 1097. (Right) Original, maximum redundant, and maximum redundant printed spectra. For the redundant spectra, green was increased 28% area coverage. See Appendix B sample MR-5a (original) and MR-5b (spectrally redundant printed).

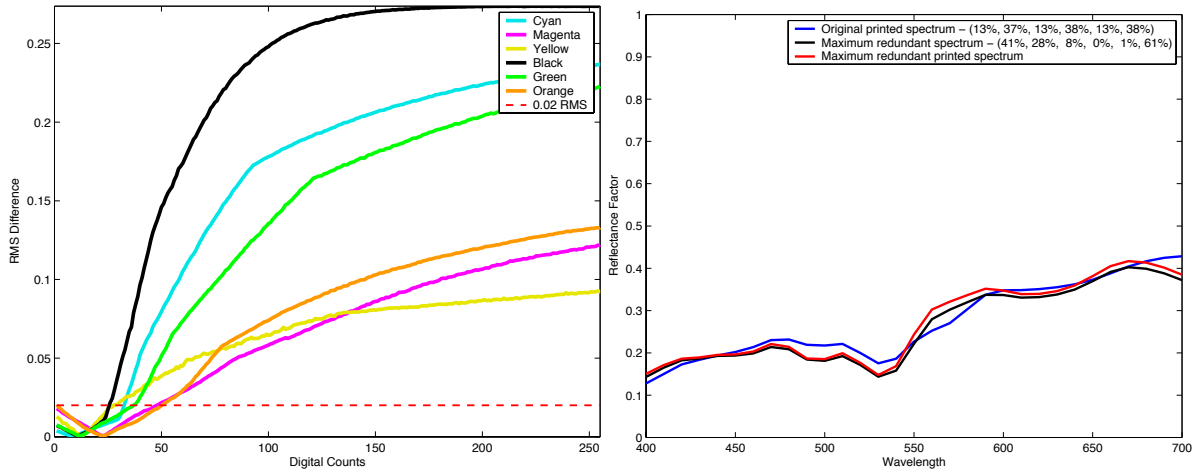


Figure 6-7. (Left) Spectral match ink variability profile for midpoint 274. (Right) Original, maximum redundant, and maximum redundant printed spectra. For the redundant spectra, orange was increased 23% area coverage. See Appendix B sample MR-6a (original) and MR-6b (spectrally redundant printed).

Table 6-1 shows the spectral RMS error, and ΔE_{00} under illuminant D65 and illuminant A using the 1931 2-degree observer for the printed patches of the original and maximum spectrally redundant area coverages.

Table 6-1. Spectral RMS differences between the original, maximum redundant estimated and maximum redundant printed spectra. Colorimetric differences are shown between the original printed spectra and maximum redundant printed spectra.

Corresponding Figure	Original/Maximum Redundant Estimated RMS	Original/Maximum Redundant Printed RMS	ΔE_{00} D65	ΔE_{00} A
Figure 6-2	0.020	0.018	0.73	1.26
Figure 6-3	0.020	0.021	0.81	1.17
Figure 6-4	0.018	0.019	5.17	4.61
Figure 6-5	0.020	0.031	3.22	3.06
Figure 6-6	0.020	0.038	3.67	3.19
Figure 6-7	0.020	0.023	1.44	2.29

Large RMS differences are found for the spectra shown in Figures 6-5 and 6-6 between the two RMS values shown in Table 6-1. This was most likely caused by interpolation errors in the characterization LUT and print-to-print variability.

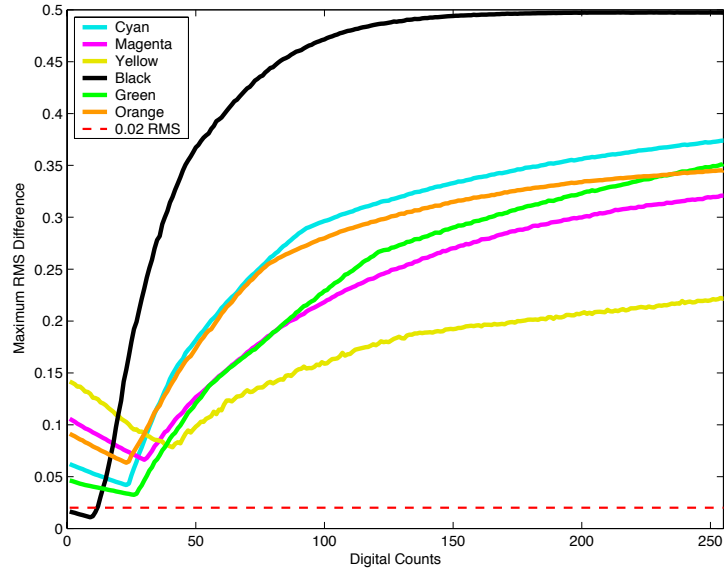


Figure 6-8. Maximum error differences for all 4,096 midpoints.

The maximum RMS difference obtained out of all the 4,096 midpoints for each ink at every digital count value is shown in Figure 6-8. At zero digital counts for each ink curve, the amount of RMS error calculated is as if an ink was completely removed from the system. If the yellow ink were removed, the analysis shows that the system would have the greatest difficulty matching at least one spectrum in the midpoint dataset. Alternatively, if black were removed, the system would be able to match all the midpoints within a spectral RMS tolerance of 0.02. This means that for the analyzed printer, black does not add any increase to the spectral gamut for a RMS tolerance of 0.02 for the midpoint dataset.

6.2 Ink Variability Density Maps

Using an RMS tolerance of 0.02, density maps were created for all 4,096 midpoint ink combinations to show where high ink variability exists. These are shown in Figures 6-10 through 6-15. Each square in the figures is associated with a CMYKGO midpoint combination.

The color bar at the right of each figure indicates the area coverage range that will match the original spectrum within a spectral RMS tolerance of 0.02. Figure 6-9 is provided as an explanation of how to interpret the density maps. The MATLAB code used to create the maps is included in Appendix A (A-3).

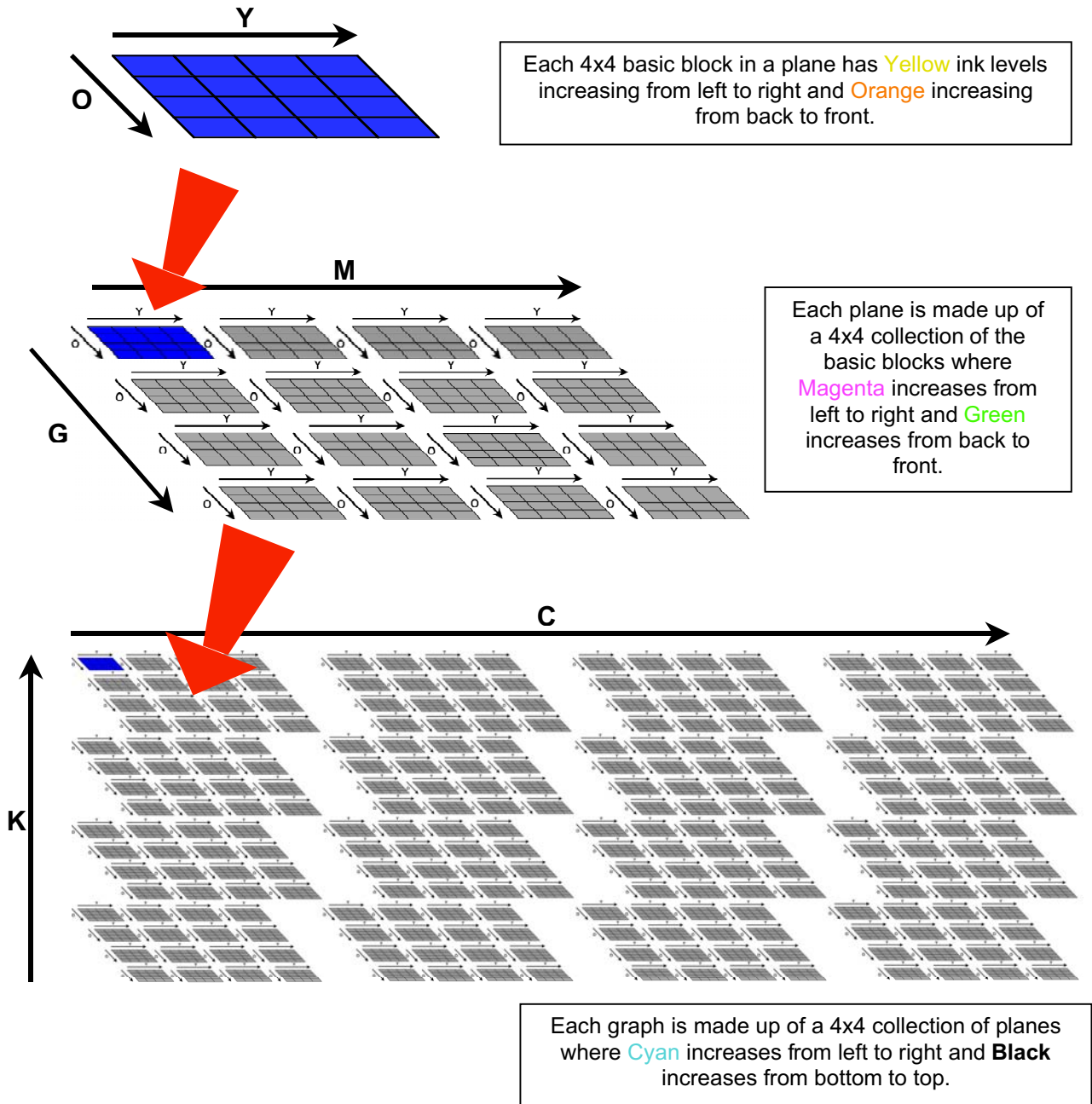


Figure 6-9. Visualization of how to interpret the ink positions in Figure 6-10 through Figure 6-15. The ink levels are arranged with respect to original ink area coverages.

7 LUT NODE ANALYSIS

7.1 *Ink Variability Results*

To further understand how prevalent spectrally stable ink-variability is throughout ink space, it was necessary to go beyond the midpoint analysis. The disadvantage of the midpoint dataset is that all patches are printed with at least 12.5% area coverage for all six inks. To analyze spectra associated with individual inks and other ink combinations with fewer than six inks participating, investigations on additional ink/spectra combinations were performed. For that purpose, two subsamplings of the 15,625-node characterization LUT were developed.

The first subset consisted of all LUT nodes with a luminance factor greater than 25. This was calculated using illuminant D65 and the 1931 2-degree observer. The second subsampling was a six-ink factorial division of the ink space that consisted of 3^6 or 729 samples. These samples were described by the percent area coverages of 0%, 50%, and 100%.

Figures 7-1 through 7-6 are based on the first subsampling described. They are similar to Figures 6-2 through 6-7 produced for the midpoint dataset in that the left side of the figures shows the spectral match ink variability profile plots and the right of the figures show the same types of reflectance curves. The blue curve is associated with the measured spectral reflectance of the original digital counts of the CMYKGO LUT node. The black curve is the maximum redundant spectrum resulting from the digital counts associated with the largest change in the indicated ink that maintains the original spectrum within a 0.02 RMS spectral difference factor. The red curve is the measured spectral reflectance of the maximum redundant printed CMYKGO digital counts. The printed samples discussed in Figures 7-1 through 7-6 are in Appendix C.

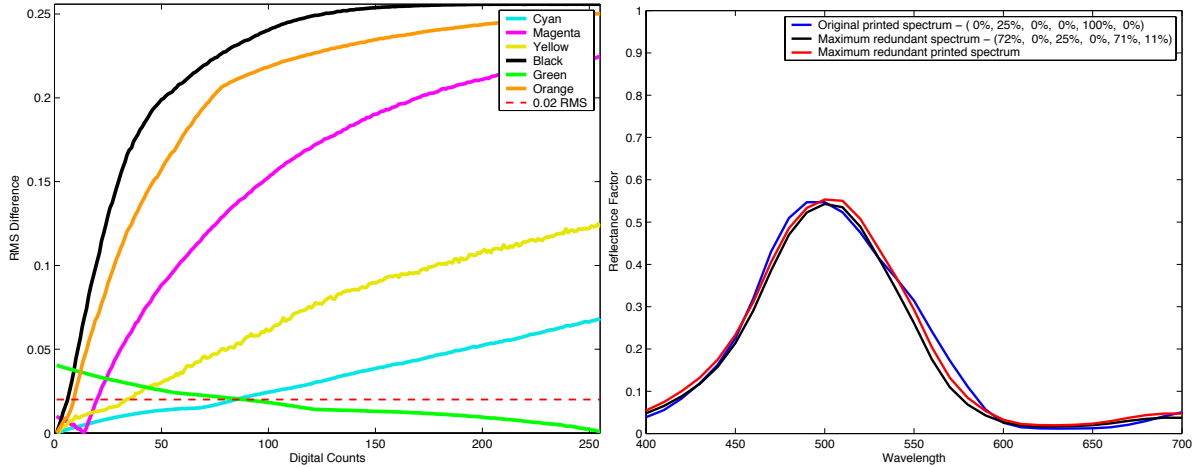


Figure 7-1. (Left) Spectral match ink variability profile for LUT node 646. (Right) Original, maximum redundant, and maximum redundant printed spectra. For the redundant spectra, cyan was increased 72% area coverage. See Appendix C sample LR-1a (original) and LR-1b (spectrally redundant printed).

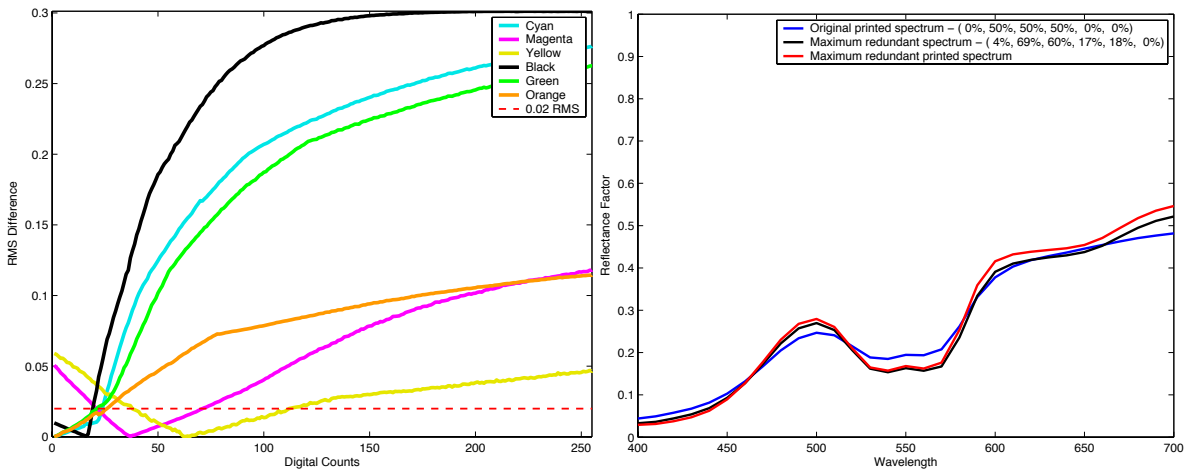


Figure 7-2. (Left) Spectral match ink variability profile for LUT node 1551. (Right) Original, maximum redundant, and maximum redundant printed spectra. For the redundant spectra, magenta was increased 19% area coverage. See Appendix B sample LR-2a (original) and LR-2b (spectrally redundant printed).

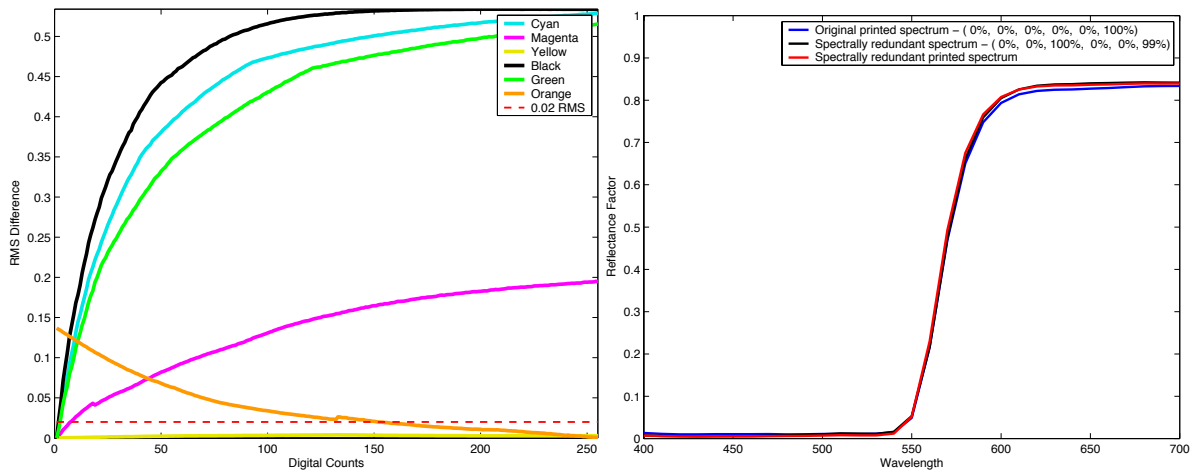


Figure 7-3. (Left) Spectral match ink variability profile for LUT node 5. (Right) Original, maximum redundant, and maximum redundant printed spectra. For the redundant spectra, yellow was increased 100% area coverage. See Appendix C sample LR-3a (original) and LR-3b (spectrally redundant printed).

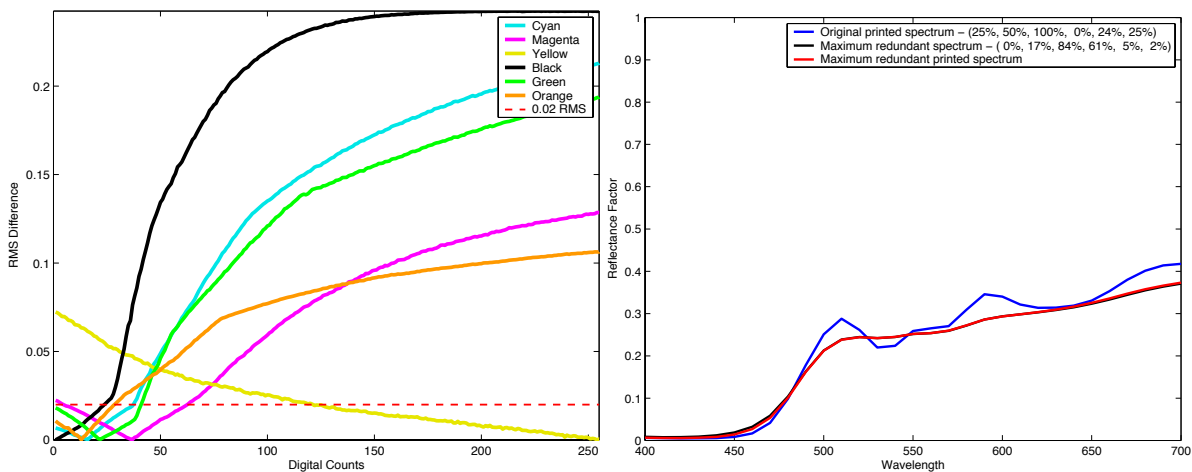


Figure 7-4. (Left) Spectral match ink variability profile for LUT node 4882. (Right) Original, maximum redundant, and maximum redundant printed spectra. For the redundant spectra, black was increased 61% area coverage. See Appendix C sample LR-4a (original) and LR-4b (spectrally redundant printed).

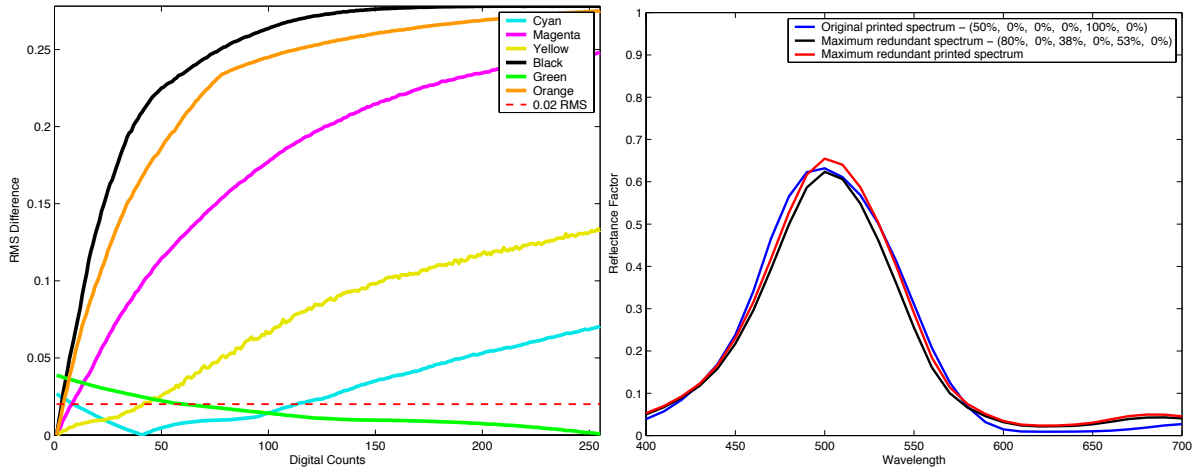


Figure 7-5. (Left) Spectral match ink variability profile for LUT node 6271. (Right) Original, maximum redundant, and maximum redundant printed spectra. For the redundant spectra, green was decreased 47% area coverage. See Appendix C sample LR-5a (original) and LR-5b (spectrally redundant printed).

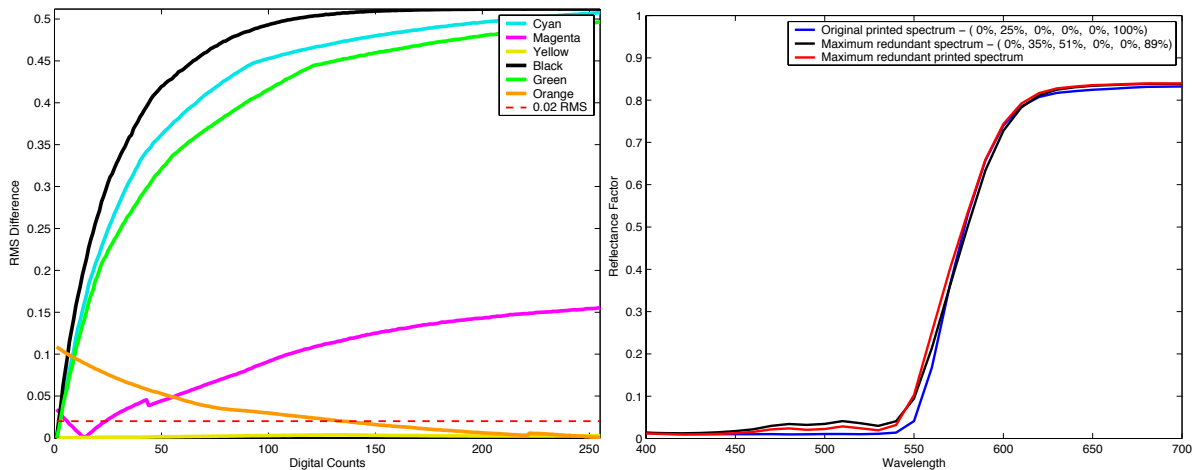


Figure 7-6. (Left) Spectral match ink variability profile for LUT node 630. (Right) Original, maximum redundant, and maximum redundant printed spectra. For the redundant spectra, orange was decreased 11% area coverage. See Appendix C sample LR-6a (original) and LR-6b (spectrally redundant printed).

Table 7-1 shows the spectral RMS error, and ΔE_{00} under illuminant D65 and illuminant A using the 1931 2-degree observer for the printed patches of the original and model estimated area coverages.

Table 7-1. Spectral RMS differences between the original, maximum redundant estimated and maximum redundant printed spectra. Colorimetric differences are shown between the original printed spectra and maximum redundant printed spectra.

Corresponding Figure	Original/Maximum Redundant Estimated RMS	Original/Maximum Redundant Printed RMS	ΔE_{00} D65	ΔE_{00} A
Figure 7-1	0.020	0.018	0.60	0.79
Figure 7-2	0.020	0.028	2.30	2.47
Figure 7-3	0.003	0.001	2.41	2.05
Figure 7-4	0.019	0.026	1.95	1.86
Figure 7-5	0.020	0.021	1.10	1.57
Figure 7-6	0.020	0.022	2.44	1.65

Larger RMS differences are found for the spectral reflectances shown in Figures 7-2 and 7-4 between the original and maximum redundant estimated spectra and the original and maximum redundant printed spectra. This is most likely caused by interpolation errors in the characterization LUT and print-to-print variability. The colorimetric differences for all the figures are relatively small even though the spectral RMS difference is at or greater than the tolerance level.

Figures 7-7 through 7-15 are based on the 3^6 factorial division of the ink space described previously. Figure 7-7 illustrates the maximum RMS difference obtained out of all the 729 LUT nodes when an ink was constrained at each digital count value.

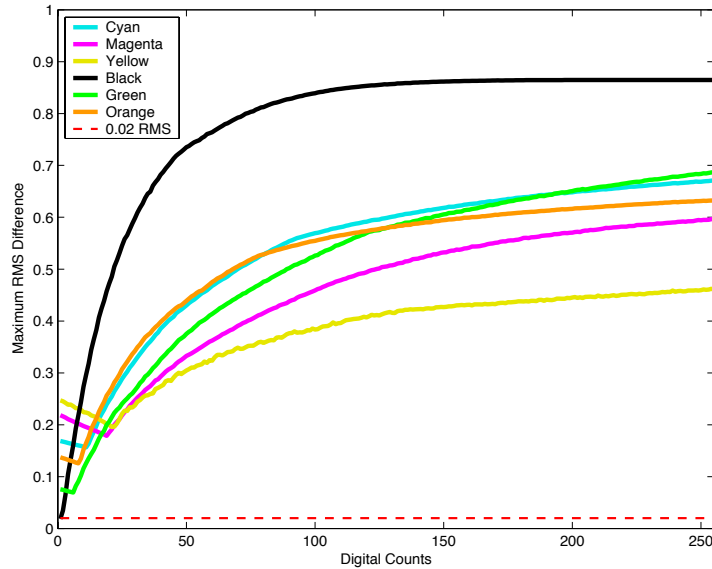


Figure 7-7. Maximum error differences for the 729 LUT node samples.

The results shown in Figure 7-7 are similar to the results found for the midpoint dataset shown in Figure 6-8. It shows that for black constrained to zero digital counts, the maximum spectral RMS difference for this dataset is below a spectral RMS tolerance of 0.02.

7.2 Ink Variability Density Maps

Using an RMS tolerance of 0.02, density maps were plotted for all 729 LUT node ink combinations to show where high ink variability exists. These are shown in Figures 7-8 through 7-13. These plots can be read similarly to the plots shown for the midpoint dataset except that each basic block is a 3x3 instead of a 4x4 and there are only 3 planes and 3 graphs for each ink. Refer to Figure 6-9 for an explanation of how to read the plots. Because of the coarse factorial sampling of ink space, non-monotonous color changes between neighbors are apparent. The MATLAB code used to create the maps is included in Appendix A (A-4).

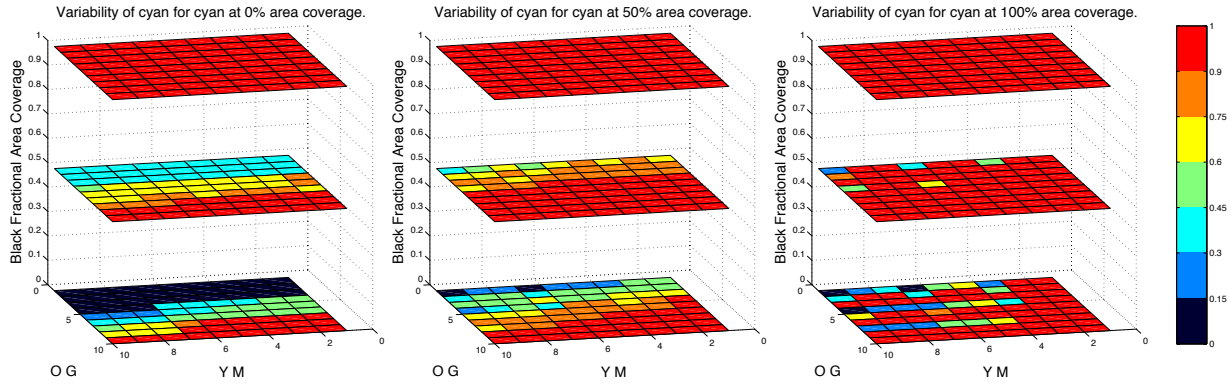


Figure 7-8. Cyan spectrally stable ink variability density map. The color bar indicates the range of cyan area coverage that will match the original spectrum within a RMS tolerance of 0.02.

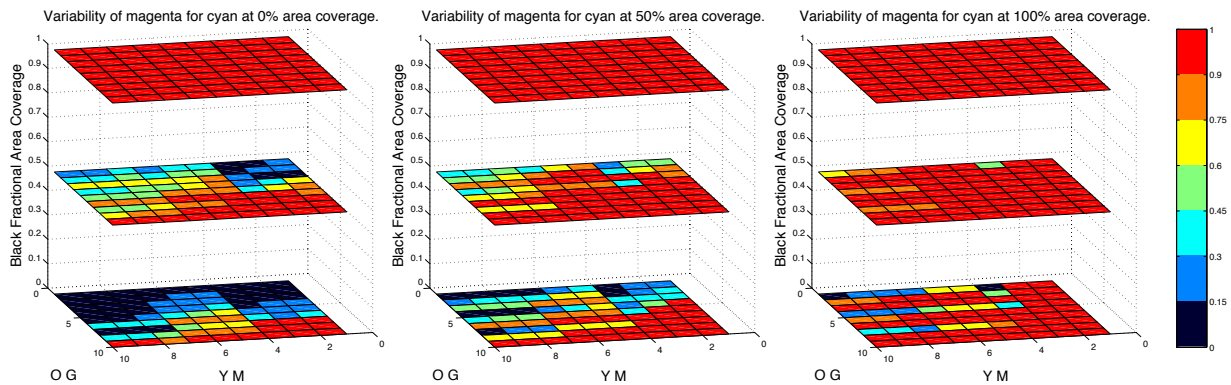


Figure 7-9. Magenta spectrally stable ink variability density map. The color bar indicates the range of magenta area coverage that will match the original spectrum within a RMS tolerance of 0.02.

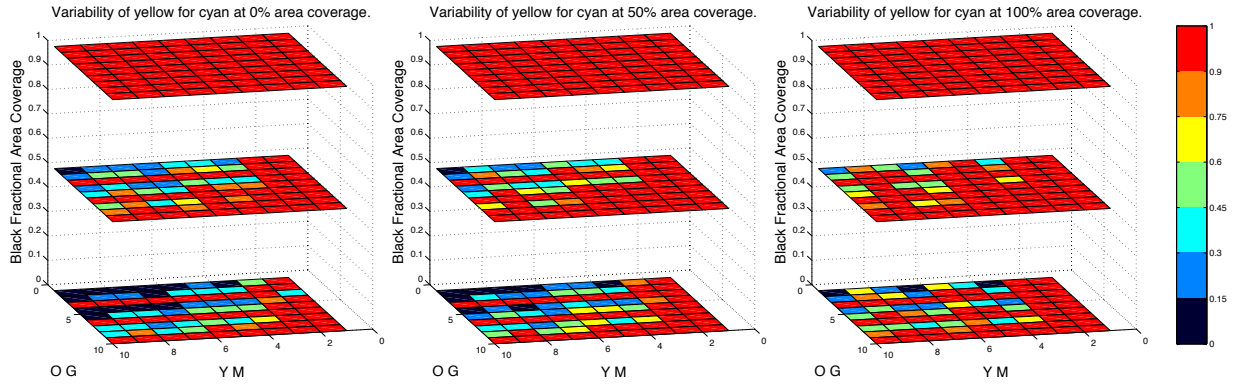


Figure 7-10. Yellow spectrally stable ink variability density map. The color bar indicates the range of yellow area coverage that will match the original spectrum within a RMS tolerance of 0.02.

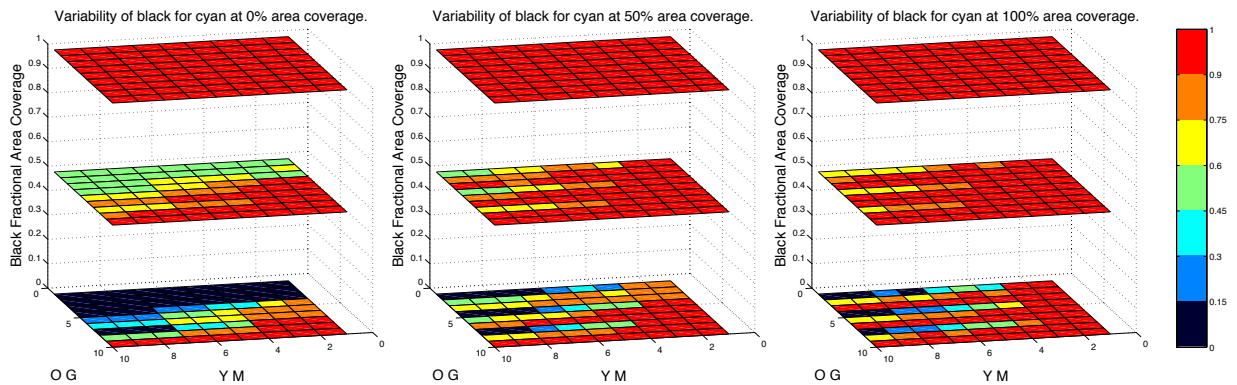


Figure 7-11. Black spectrally stable ink variability density map. The color bar indicates the range of black area coverage that will match the original spectrum within a RMS tolerance of 0.02.

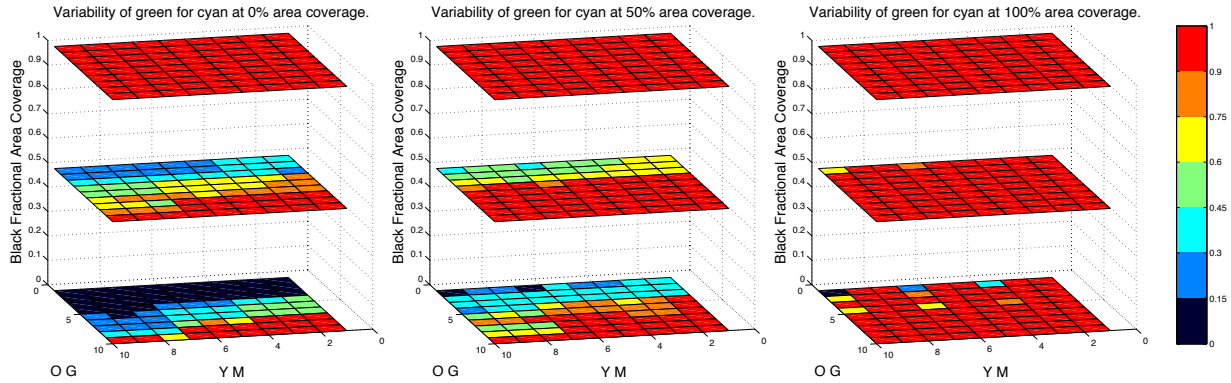


Figure 7-12. Green spectrally stable ink variability density map. The color bar indicates the range of green area coverage that will match the original spectrum within a RMS tolerance of 0.02.

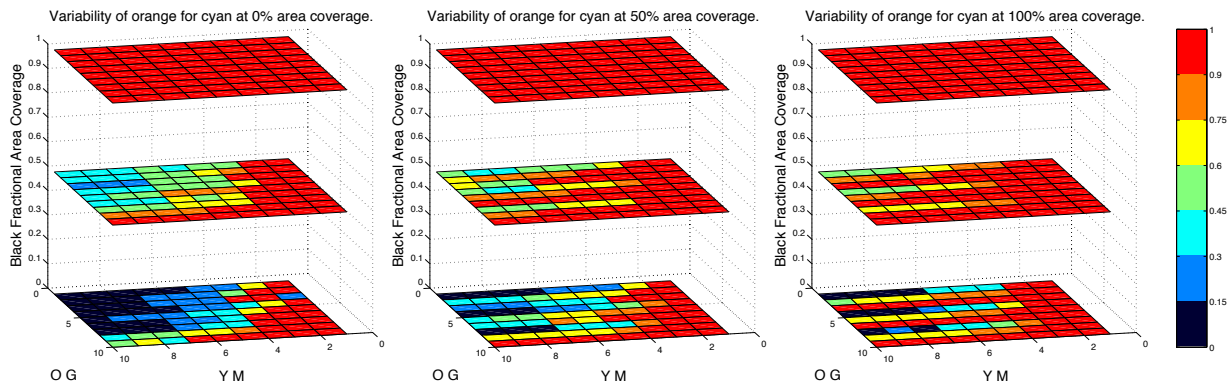


Figure 7-13. Orange spectrally stable ink variability density map. The color bar indicates the range of orange area coverage that will match the original spectrum within a RMS tolerance of 0.02.

Table 7-2 summarizes the ink variability density maps. This summary concludes that when specific individual inks or inks in combination are present at high area coverages, it is possible for an ink to be highly variable and maintain a RMS tolerance of 0.02. The results of the factorial LUT sampling support the results found in the midpoint sampling.

Table 7-2. Summary of Figure 7-8 through Figure 7-13.

Figure	Highly Variable	When These Inks Are Present In High Amounts
Figure 7-8	Cyan	Black Cyan & Orange Green & Orange Cyan & Magenta & Yellow
Figure 7-9	Magenta	Black Cyan & Orange Green & Orange Cyan & Magenta & Yellow
Figure 7-10	Yellow	Black Orange Magenta & Yellow
Figure 7-11	Black	Black Cyan & Orange Green & Orange Cyan & Magenta & Yellow
Figure 7-12	Green	Black Cyan Green & Orange
Figure 7-13	Orange	Black Cyan & Orange Magenta & Yellow Magenta & Green

7.3 Colorimetric Evaluation Without The Black Ink

As shown in Figure 7-7, black for this system no longer adds another degree of spectral matching freedom if spectral RMS were selected as a spectral matching metric with a tolerance of 0.02.

Colorimetric differences in ΔE_{00} units were calculated for the 729 LUT node sub sampling between the original measured midpoint spectral reflectance and the model predicted spectral reflectance with black constrained to zero digital counts. Figure 7-14 is a histogram of ΔE_{00} colorimetric differences using the 2-degree observer and illuminant D65 (left) and illuminant A (right). Three hundred eighty four original LUT node ink combinations that pooled or blotted

when printing were not included in this evaluation because these spectral reflectances relied on statistical prediction.

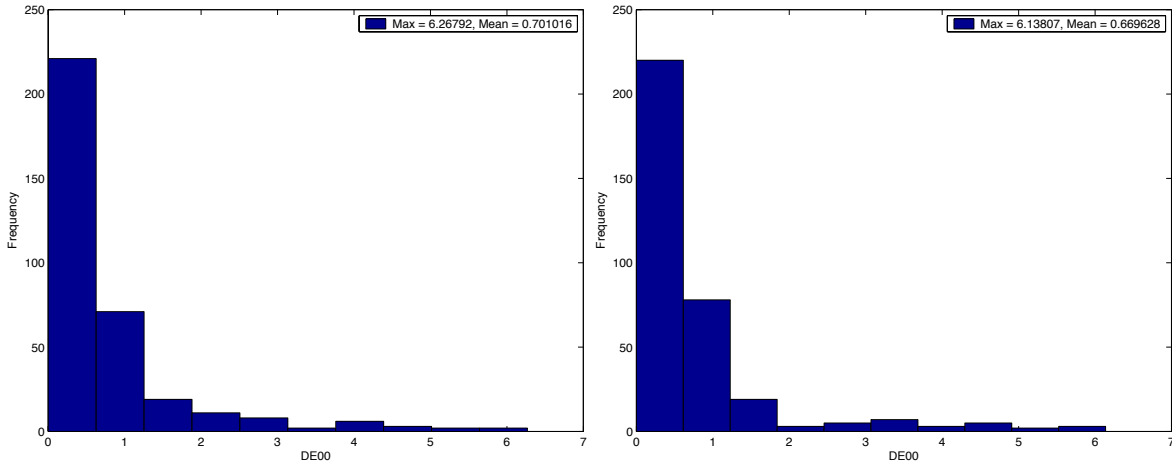


Figure 7-14. Histogram of colorimetric differences in ΔE_{00} units when matching the midpoint spectral reflectances with black at zero digital counts.

When using a spectral RMS tolerance of 0.02, a maximum ΔE_{00} of 6.3 under illuminant D65 and 6.14 under illuminant A were found. This is similar to the results found when the midpoint dataset was analyzed.

Figure 7-15 was created to show the colorimetric differences that occurred for the factorial characterization LUT sampling at a tolerance of 0.02 spectral RMS when black is removed from the system. The color bar shown at the right indicates the range of ΔE_{00} values found for this analysis. A white square indicates that the original LUT node ink combination was not printable due to ink pooling (see discussion in section 3.2).

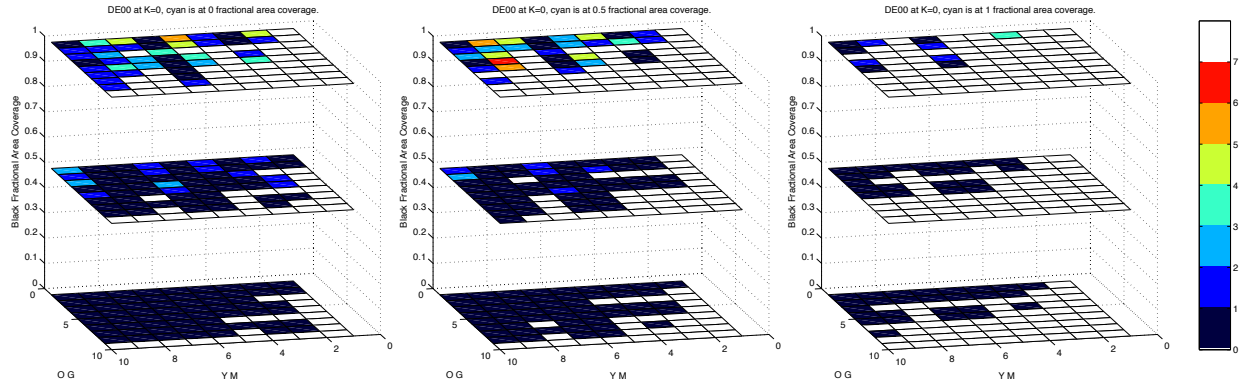


Figure 7-15. Colorimetric differences in ΔE_{00} units when matching the LUT node spectral reflectances with black at zero digital counts.

Analysis of Figure 7-15 shows that the largest colorimetric differences are found for spectra with black at high area coverages. Additional patterns cannot be interpreted because a large number of LUT nodes were not printable.

8 MIDPOINT AND LUT NODE CONCLUSIONS

The algorithm developed to uncover spectrally stable ink variability mapped out ink variability ranges for the midpoint dataset and the 3^6 factorial sampling of the 15,625-node characterization LUT. The advantage of the midpoint dataset discussed in chapter 6 is that it consists of 4,096 sampling points that closely and evenly sample colorant space. A disadvantage is that every patch has at least 12.5% area coverage for all six inks. The 3^6 LUT factorial sampling discussed in chapter 7 extends beyond the gamut associated with the midpoints. This includes individual inks at specific area coverages and inks in various combinations with fewer than six inks participating. Because of optimization time and data storage constraints, the entire characterization LUT was not analyzed. The factorial sampling coarsely represents the complete printer gamut. The datasets from chapters 6 and 7 exhibit similarities when compared with each other.

Evaluating Figure 6-8 of the midpoint dataset and Figure 7-7 of the factorial sampling shows that when black was constrained at zero digital counts, the system was able to match respective dataset spectra within a spectral RMS tolerance of 0.02. This implies that if a spectral RMS difference of 0.02 is suitable for a specific application, black does not add any increase in the spectral gamut of the evaluated printer.

When comparing the spectrally stable ink variability maps corresponding to Figures 6-10 through 6-15 of the midpoint dataset to Figures 7-8 through 7-13 of the LUT factorial sampling, many similar trends are seen. This is also evident when comparing the summarized results illustrated in Tables 6-2 and 7-2. The largest difference between the two tables is that green is highly variable when black is present at high amounts for the LUT node factorial sampling but

not for the midpoints. One explanation for this is that black was not at a high enough area coverage in the midpoint dataset for the green ink to be highly variable.

Similar trends are also seen when reviewing the ΔE_{00} colorimetric difference plots with black constrained to zero digital counts. Larger colorimetric differences are found at low reflectance factors in both datasets. These are located in the top planes of Figures 6-17 and 7-15. As seen in Figure 5-4, black is somewhat spectrally flat and the chromatic inks had increased difficulty in matching this characteristic. This occurrence also suggests that comparing spectra in linear reflectance space may not have been a good choice. Because the spectra associated with the top planes have a low reflectance factor, small spectral RMS differences can relate to large colorimetric differences. Better results may have been obtained if an alternative spectral difference metric not susceptible to this problem were used.

9 SPECTRAL ERROR METRIC INVESTIGATION

Building a database containing pointers to many spectrally similar ink combinations is important for designing psychophysical experiments for visually evaluating spectral difference metrics. Because the algorithm developed to uncover spectral redundancy within a multi-ink printer is independent of the spectral difference metric, any metric can be evaluated or compared to other spectral difference metrics with respect to visual validity.

After discovering that black could be removed from the evaluated printer system without introducing a spectral RMS error greater than 0.02, efforts focused on determining how these differences would manifest colorimetrically. Reviewing the midpoint dataset colorimetric difference plots shown in Figure 6-17 revealed that differences greater than five ΔE_{00} colorimetric units occurred for darker reflectance spectra that were well within the 0.02 spectral RMS tolerance.

To verify that an observer would agree with the amount of visual difference predicted by ΔE_{00} , the original and spectrally redundant model predicted reflectances were printed. Twenty-four light colors and twenty-four dark colors were chosen for visual comparison. The light colors had spectra with a luminance factor greater than or equal to 25. This included six midpoints, six lookup table nodes and an associated spectrally redundant ink combination within a 0.02 spectral RMS tolerance. The dark colors had a luminance factor of approximately 3. They were chosen from the midpoint dataset based on the large colorimetric difference that occurred when the midpoint dataset spectral reflectances were matched without using the black ink. Prints of the midpoints and LUT nodes with a luminance factor greater than 25 are shown in Appendix B and C respectively. Prints of the dark midpoint color patches are in Appendix D. Using the model predicted and measured spectra obtained from the printed samples, the spectral

RMS difference and associated ΔE_{00} using the 1931 2-degree observer and illuminant D65 of the light colors and dark colors were compared. The results are shown in Table 9-1.

Table 9-1. Model predicted and measured spectral and colorimetric differences for several light colors and dark colors.

	Dark Colors (Appendix B)				Light Colors (Appendix C)			
	Predicted		Measured		Predicted		Measured	
	RMS Difference	ΔE_{00}	RMS Difference	ΔE_{00}	RMS Difference	ΔE_{00}	RMS Difference	ΔE_{00}
Mean	.0051	5.41	.0071	4.19	.0186	2.36	.0229	2.15
Maximum	.0080	5.85	.0110	6.35	.0278	5.82	.0374	5.17
Std. Dev.	.0019	0.23	.0030	1.11	.0056	1.38	.0071	1.37

Table 9-1 illustrates that although the mean spectral RMS differences for the model predicted and printed samples was 0.0051 and 0.0071 respectively for the dark colors, an average ΔE_{00} of 5.41 and 4.19 was calculated. Alternatively for the light colors, the RMS difference was approximately equal to the spectral difference tolerance level of 0.02 and the average colorimetric differences were much smaller than that of the dark colors. When viewing the color patches in Appendix D, larger colorimetric differences can be seen. For example, the ΔE_{00} between printed samples MDE-6a and MDE-6b is 6.34. When viewing the patches in a light booth under simulated D65, a large color difference can be seen although the spectral RMS difference is only 0.004. In comparison, the ΔE_{00} between the printed samples MR-2a and MR-2b in Appendix B is 0.81 even though the spectral RMS difference is 0.021. This supports ΔE_{00} in that it is tracking well with visual perception whereas spectral RMS does not as luminance changes.

This experiment illustrates the advantage of using the techniques to uncover spectral redundancy to evaluate spectral difference metrics. First, the ability to evaluate spectrally similar samples showed that spectral RMS difference does not correlate well with ΔE_{00} . Second,

by printing spectrally similar samples, spectral difference metrics can be compared to visual responses.

10 THE INFLUENCE OF SPECTRAL REDUNDANCY ON SPECTRAL COLOR MANAGEMENT

Research in the field of spectral hardcopy output has overcome many hurdles over the past years. Publications have described the process of using multiple printing inks to make reasonable spectral matches, and have evaluated forward models that relate digital counts to spectra.^{1,2,5,7} Investigations focusing on the implementation of the inverse model relating spectral reflectance or spectral correlates to digital counts have also been conducted. A computationally feasible method reduced the dimensionality of 31-band spectral sampling to a 6-ink printer via a multi-dimensional LUT by deriving weightings from a fixed set of spectral reflectances obtained from the input spectra.⁴ An experiment was designed to further explore the inverse transform by looking at the importance of digital count consistency between adjacent nodes in a lookup table that converts from spectra to digital counts.

The presence of spectrally stable ink variability suggests that when building a spectral transformation lookup table, there will often be situations where multiple digital count combinations could potentially be assigned to adjacent spectral nodes without causing spectral error at the nodes themselves to rise. Unless adjacent nodes are carefully evaluated for consistency, colorimetric error could be amplified when interpolating through the lookup table.

10.1 Spectral Color Management

The three main components of a color reproduction system are image capture, image processing, and image output. Accurate color reproduction can only be achieved when the image processing phase is informed of the image capturing and image rendering device characteristics. The

industry standard ICC color management platform relates a source image to an output rendering device via the source profile and the destination profile. Both profiles provide data that relate the source and destination digital counts to a three-dimensional color space. Well known are the metameric characteristics between the original and reproduced image using a colorimetric approach.

The goal of spectral color management is to accurately reproduce the spectral reflectance of the original imaged scene. The advantage of a spectral match is that a color match will be maintained for all observers across any illumination. The spectral color reproduction chain would differ from ICC in that the source and destination profiles would relate digital counts to spectra. Typically an ICC profile is implemented by concatenating the source and destination profiles into a direct lookup table between input digital counts and destination digital counts. This is computationally impossible in spectral color management because the destination profile that relates spectral reflectance to output digital counts would become extremely large. Implementation of the spectral color management workflow requires a stage where spectra are decomposed into a set of spectral correlates that are used as indices into the destination profile lookup table.⁴ A diagram of a realized spectral color management workflow is shown in Figure 10-1.

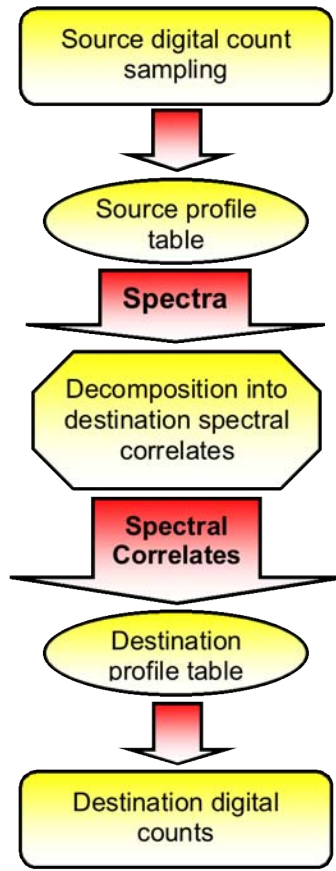


Figure 10-1. Realized spectral color management workflow.

The efforts of this research are focused on the influence of spectrally stable ink variability when developing the destination profile table.

10.2 The Influence of Spectrally Stable Ink Variability on Multi-Dimensional Lookup Tables

Typically, the forward printer model that relates digital counts to spectra is not easily invertible. To populate a multi-dimensional lookup table that relates spectra to printer digital counts, search methods are used to accurately guess the digital counts that produce a requested spectral reflectance. Spectrally stable ink variability can cause unexpected results at this step in the

spectral color management chain. Figure 10-2 shows the process for populating a multi-dimensional lookup table that relates spectra to digital counts. This diagram assumes that the dimensionality of the input spectra have been reduced and the multi-dimensional lookup table will relate spectral correlates to printer digital counts.

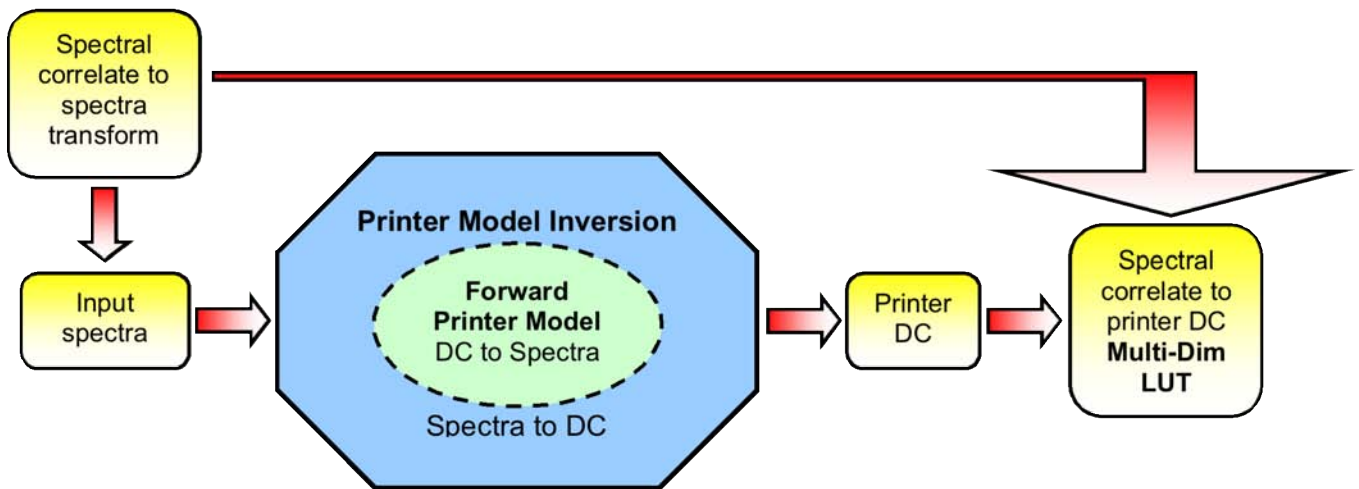


Figure 10-2. The process needed to produce a spectral reflectance to digital count multi-dimensional lookup table.

Because of spectrally stable ink variability, it is possible that a variety of digital count combinations could be used to match a given spectrum. The consequence of this is that adjacent nodes in spectral space may have drastically different six-ink digital count combinations. The digital count inconsistencies result in unpredicted spectra when interpolating between adjacent nodes.

10.3 Experimental

To demonstrate the outcome when adjacent LUT nodes are inconsistent in output digital counts, the results of the spectrally stable ink variability analysis on the midpoint dataset were used. For each node in the midpoint dataset, its maximum redundant ink pair was determined for each ink from the largest digital count distance an ink could be moved while maintaining the measured spectral reflectance within a 0.02 spectral RMS. Therefore, every node in the midpoint dataset had six maximum redundant ink pair sets where each corresponded to one of the six inks.

Two interpolations were implemented. First, spectral interpolations were computed between an original six-ink combination at a node and the original six-ink combinations at every adjacent node. Second, interpolations were made between a node's maximum redundant ink pairs and the adjacent node. The interpolation distances selected were 25%, 50%, and 75% of the entire distance between the nodes. Printed examples are shown in Appendix E. When comparing the printed interpolation ramps shown in Appendix E, the top nodes of a pair labeled “#a”, “#b” have spectrally similar spectra, and the bottom nodes have exactly the same digital count combinations. Differences in spectra for these nodes can be attributed to system variability.

Table 10-1 shows for all twelve pairs in Appendix E labeled “MIL-#a”, “MIL-#b”, the ΔE_{00} between the nodes with consistent digital counts and the nodes with inconsistent digital counts. Illuminant D65 and the 1931 2-degree observer were used in the calculation.

Table 10-1. Colorimetric differences that occur when a node is substituted with a spectrally similar but different digital count combination. Note the bottom nodes were designed to have the same CMYKGO digital count combinations.

Sample pair	ΔE_{00}				Bottom Nodes
	Top Nodes	25% Interpolation	50% Interpolation	75% Interpolation	
MIL-1a, MIL-1b	1.82	7.03	7.86	3.96	0.11
MIL-2a, MIL-2b	2.55	8.64	9.17	5.26	0.08
MIL-3a, MIL-3b	0.69	5.55	6.42	3.79	0.06
MIL-4a, MIL-4b	2.10	5.88	7.14	3.96	0.03
MIL-5a, MIL-5b	1.76	6.35	8.20	4.38	0.08
MIL-6a, MIL-6b	1.04	4.58	5.76	3.59	0.09
MIL-7a, MIL-7b	1.56	5.64	6.44	3.49	0.08
MIL-8a, MIL-8b	1.60	5.21	6.61	5.59	0.28
MIL-9a, MIL-9b	1.56	4.15	6.24	5.10	0.21
MIL-10a, MIL-10b	1.64	5.54	7.43	4.39	0.11
MIL-11a, MIL-11b	1.84	8.45	6.04	3.81	0.06
MIL-12a, MIL-12b	1.37	4.49	4.55	2.83	0.10

The results in Table 10-1 show that if a node with consistent digital counts to its neighbor in a LUT is replaced with a spectrally similar node at a 0.02 spectral RMS difference tolerance, large interpolation errors can result.

Colorimetric plots in the CIELAB a^* , b^* plane were created for the Appendix E sample pairs labeled MIL-5a, MIL-5b and MIL-10a, MIL-10b illustrating the error. These are shown in Figure 10-3.

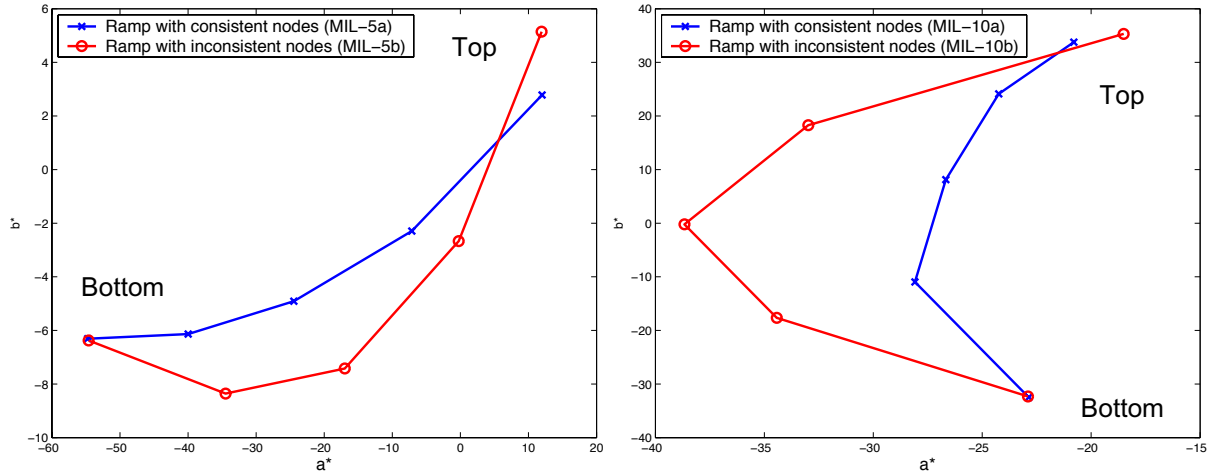


Figure 10-3. Colorimetric plots associated with the Appendix E sample pairs labeled MIL-5a, MIL-5b and MIL-10a, MIL-10b. The left figure corresponds to the pair labeled MIL-5a, MIL-5b.

10.4 Conclusions

Digital count consistency between nodes in a spectral color management lookup table is very important. The algorithm used to uncover spectrally stable ink variability throughout the printer gamut was effective in identifying examples of where inconsistent digital count combinations at spectrally adjacent nodes could cause troublesome colorimetric results. Algorithms for selecting consistent adjacent nodes when building lookup tables for use in spectral reproduction must be designed to minimize this occurrence.

11 SPECTRALLY TRANSLUCENT WATERMARKING

Analyzing the spectral redundancy within a printing system opens the door to new applications such as spectrally translucent watermarking. The methods developed to uncover spectral redundancy can be used to embed information inside an image. The embedded information may be slightly visible or invisible depending on the application. This can be applicable to the field of steganography or image security.

The purpose of steganography is to communicate information by undetectably embedding it in an image. Steganalysis involves the detection and extraction of such images. Associated with a steganographic transmission is an embedding algorithm and an extraction algorithm. The embedding algorithm slightly alters the original image to accommodate the hidden data. The extraction algorithm allows the hidden information to be retrieved.

The field of steganography is becoming increasingly important since the circulation of digital images is relatively straightforward via the Internet and E-mail. Many steganographic and steganalysis techniques have been developed.¹⁶ Data hiding techniques related to halftoned images have focused on altering the halftone pattern to embed the hidden information.^{17,18} Other steganographic algorithms have evaluated watermarked images based on the total color difference change at a pixel after the watermark signal has been embedded.¹⁹ The methods created to uncover spectral redundancy can be used to make a hidden image undetectable without knowing the decryption technique.

Exploiting spectral redundancy in image security can help protect image propriety. Embedding a watermark that is all but invisible from one viewing angle, but clearly visible from another can easily establish image ownership. The advantage of spectrally stable watermarking

is that it transcends colorimetric differences and embeds the information based on the underlying spectral reflectance at a given pixel. To illustrate the significance of watermarking techniques that use spectrally stable ink variability, information was embedded into three images with varying levels of complexity.

11.1 Level 1: Embedding Information In A Uniform Color Patch

The goal of this experiment was to hide information into a uniform color patch. Using the results returned from the spectrally stable multi-ink variability analysis, two distinct six-ink combinations were selected that produced the same spectral reflectance within a 0.01 spectral RMS difference.

A binary image was created using Adobe Photoshop® with the text “MCSL”. The image is shown in Figure 11-1.

The image shows the text "MCSL" in a large, bold, black, sans-serif font. The letters are thick and have a slightly irregular, hand-drawn appearance. The text is centered horizontally and occupies most of the width of the page.

Figure 11-1. Text image embedded in a uniform color patch.

One set of six-ink digital counts was assigned to the text and the other six-ink combination was assigned to the rest of the image. The print of this image is in Appendix F pages F-3 through F-4.

The two spectra used to create the uniform color patch were measured and the plot is shown in Figure 11-2.

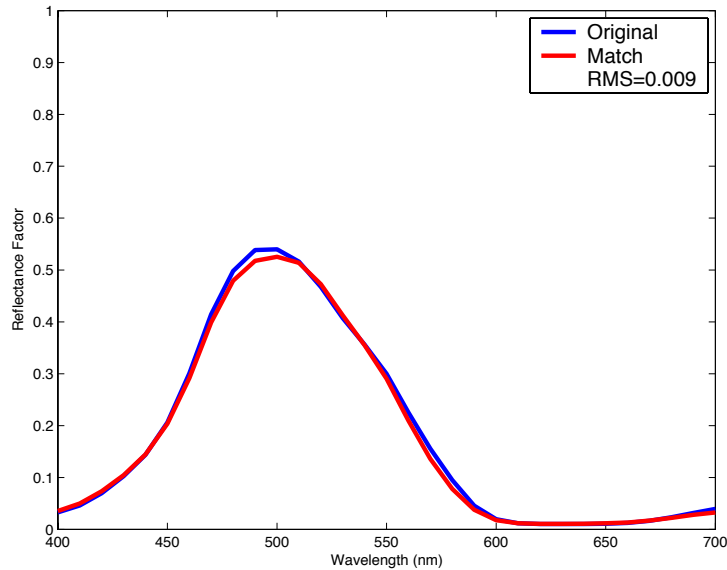


Figure 11-2. The measured spectral reflectances of the two six-ink digital count combinations.

The original spectral reflectance was created using the digital count combination of C=0, M=13, Y=0, K=0, G=255, O=0, and the matched spectral reflectance with C=24, M=5, Y=3, K=0, G=218, O=3.

When the uniform color patch is viewed under simulated illuminant D65 in a light booth, it is very difficult to see the hidden text. If the color patch is viewed under other illuminants, a very small color difference can be detected and the text can be seen. Although different inks are being used for the text and surround, the halftone pattern is not revealing the hidden information. If the image is viewed at the specular angle for all illuminants, the text can be seen because of changes in ink gloss characteristics. When the ink separations are printed, it is easy to see the text hidden in the color patch. The MATLAB code developed for this experiment is in Appendix A (A-5).

11.2 Level 2: Simple Image Watermarking

For this experiment, the binary image shown in Figure 11-1 was embedded in a simple image. The simple image shown in Figure 11-3 was first created in Adobe Photoshop® as a grayscale image and then quantized into six gray level values.

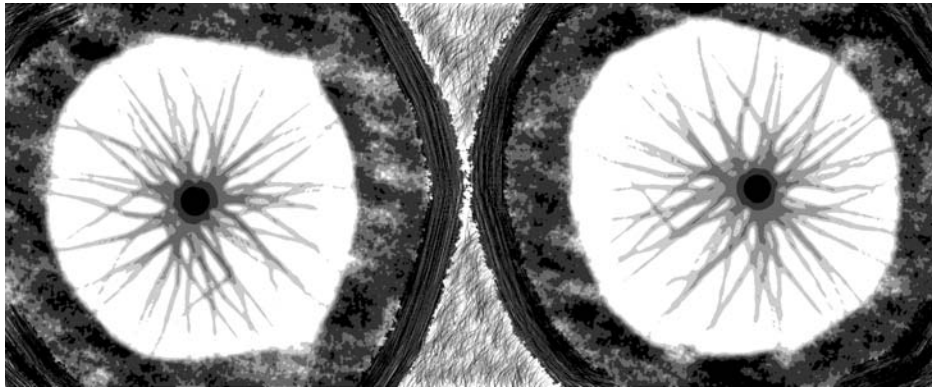


Figure 11-3. Image used in simple image embedding experiment.

Six midpoint digital count combinations were selected as well as six spectrally redundant digital count combinations. The digital count combinations are shown in Table 11-1.

Table 11-1. Six midpoint six-ink combinations and six spectrally redundant six-ink combinations used for the simple image embedding.

Midpoint and Spectrally Redundant 6-ink Combinations	Cyan Digital Counts	Magenta Digital Counts	Yellow Digital Counts	Black Digital Counts	Green Digital Counts	Orange Digital Counts
Midpoint 2249	61	6	186	3	83	5
2249 Redundant	91	0	199	1	48	9
Midpoint 780	7	131	11	3	83	126
780 Redundant	14	93	12	14	48	150
Midpoint 1291	26	22	11	3	83	51
1291 Redundant	51	12	16	3	48	58
Midpoint 2057	61	6	11	3	83	5
2057 Redundant	89	2	19	0	48	10
Midpoint 4076	7	22	186	11	83	126
4076 Redundant	31	1	253	12	48	145
Midpoint 1802	26	131	11	3	83	21
1802 Redundant	50	131	19	3	48	17

The spectrally redundant six-ink combinations were chosen because the model predicted spectral reflectance was less than a spectral RMS error of 0.01 from their associated midpoint spectral reflectance. The “MCSL” image was hidden in the green channel for this experiment. The print of this image is in Appendix F pages F-5 through F-7 and the MATLAB code is in Appendix A (A-6).

When viewing this image, it is extremely difficult to tell that it was watermarked. The watermark can clearly be seen when viewing the six-ink separations. As in the previous experiment, the halftoning pattern, although slightly visible at the text interface, does not reveal the information hidden in the image. If the image is viewed at the specular angle, the text is not visible. This may be due to the relatively high ink levels used to create the image.

11.3 Level 3: Complex Image Watermarking

The ability to hide information at each pixel allows the entire image to be used for watermark embedding. In this experiment, an entirely different grayscale image was embedded into a complex original image. The original image is shown in Figure 11-4.

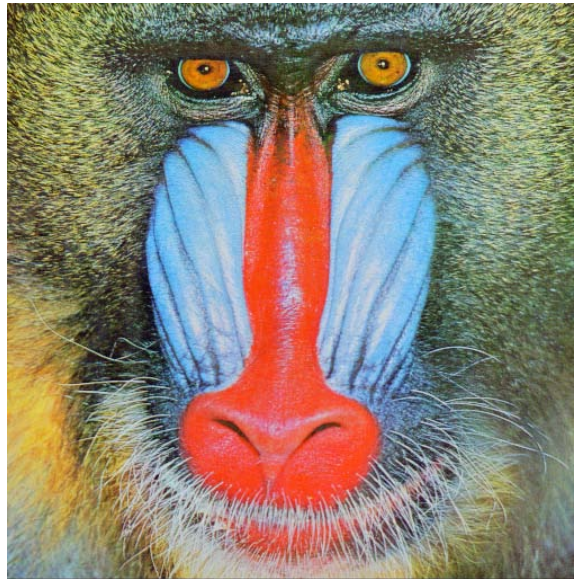


Figure 11-4. Image used in complex image embedding experiment.

Because the spectrally stable multi-ink variability was performed on the midpoint dataset and not the full digital count factorial sampling used to build the printer model, the image was quantized so that each pixel would fall on one of the midpoint dataset nodes. The grayscale image of the Rosetta stone taken by the author when visiting the British Museum was embedded within a single separation of the original image. This image is shown in Figure 11-5.



Figure 11-5. Hidden image used in complex image embedding experiment.

Based on the gray level value in the hidden image, a pixel-by-pixel analysis was used to access the spectrally redundant midpoint database of the channel that the image was to be embedded in and find the six-ink values associated with the previously minimized spectral error. To minimize the visual impact of the hidden image, an error clipping procedure was performed so that the spectral error introduced into the watermarked image would not increase above 0.02. A diagram of this procedure for an arbitrary midpoint spectral reflectance is shown in Figure 11-6.

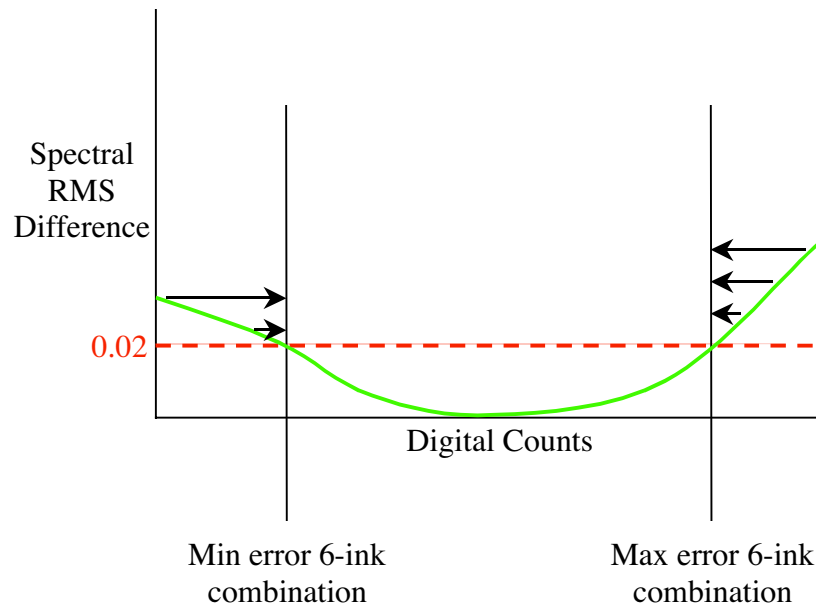


Figure 11-6. Diagram illustrating the error clipping procedure.

If a pixel in the hidden image required a digital count value that increased the original image spectral reflectance above 0.02 spectral RMS difference, it was mapped to digital count that prevented the spectral difference from increasing above the 0.02 tolerance. The original quantized image (left) and the spectrally watermarked image (right) are in Appendix F pages F-7 through F-10 and the MATLAB code is in Appendix A (A-7).

Comparing the original image to the watermarked image reveals that the procedure was successful in embedding the hidden image. Artifacts and random speckling caused by the process can be seen in uniform areas of the watermarked image, especially in the bridge of the red nose. Examining the green channel where the hidden image was embedded shows a faint shadow of the nose. This indicates that the spectral reflectances associated with the nose were very sensitive to changes in green ink levels. This probably occurred because red and green are opponent colors. An alternative spectral difference metric would likely be needed to successfully embed the image especially in the reddish areas. The watermark can be clearly

seen when the watermarked image is held to view the specular reflection off the image. This is most likely caused by the different gloss characteristics of the inks.

12 CONCLUSIONS

This research uncovered effective methods for evaluating spectrally stable ink level variability in multi-primary printers. The algorithm developed to systematically determine the multi-ink variability throughout the spectral gamut of a printer is particularly useful because any spectral difference metric can be used. For this research, spectral RMS was selected as the spectral difference metric and 0.02 spectral RMS difference as the tolerance limit. Novel six-dimensional density map displays were created using the information returned from the spectrally stable multi-ink variability algorithm. These showed how the prevalence of spectral redundancy in the tested printer changed throughout ink space.

Designed experiments exploited spectral redundancy within the analyzed printer. The first experiment applied the spectrally stable multi-ink variability analysis to evaluate spectral difference metrics. Printers that have undergone spectrally redundant analysis can be used to generate samples for comparing a visual response to a spectral difference metric.

The second experiment demonstrated the importance of spectral redundancy in spectral color management. Typical color image processing techniques use profiles consisting of sparse multi-dimensional lookup tables that interpolate between adjacent nodes to prepare an image for rendering. By design, the input space of the lookup table has consistency between adjacent nodes. A lookup table that transforms spectrally derived values to printer digital counts can be negatively impacted when the output space values between adjacent nodes are inconsistent. It was demonstrated that inconsistency between nodes in the output printer digits creates unfavorable colorimetric results when interpolating.

Finally, the analysis was used to spectrally watermark images. Three levels of complexity were developed for this technique. In the first level, a simple binary image was

embedded in a uniform color patch. By assigning two distinct sets of digital counts that produce the same spectral reflectance within a 0.01 spectral RMS difference, the hidden image was virtually undetectable at a typical viewing angle and easily seen at the specular angle.

The second level of spectral watermarking involved embedding a binary image in the green channel of a simple quantized grayscale image. Six midpoint digital count combinations and six spectrally redundant digital count combinations were selected from the midpoint analysis. Assigning the spectrally redundant six-ink combinations to the “on” position of the binary image allowed it to be hidden in the green channel. For this image, the embedded text could not be seen at the specular angle.

The third level of watermarking embedded a complex grayscale image into a complex color image. Using the information from the analysis of the midpoint dataset and implementing a new algorithm that did not allow more than 0.02 spectral RMS difference at each pixel of the original image, the grayscale image was embedded into the original image while preserving the visual and spectral integrity of the original image. At typical viewing angles the embedded image could not be seen; however, when the image was viewed at the specular angle, the image of the Rosetta stone was clearly distinguishable.

12.1 Future Research

Research in the area of spectrally stable multi-ink variability has just come to light. Alternative algorithms should be developed to uncover largely different ink combinations throughout the printer gamut that produce similar spectra. Refinement of the algorithm implemented in this research is worth pursuing because it is computational intensive and the output files are relatively large.

This thesis has touched on several important applications that are worth investigating in further detail. Assisting in the search for alternative spectral difference metrics as well as evaluating existing metrics is important. Another important research area is to develop algorithms that select consistent digital count combinations for use in multi-dimensional lookup tables that relate spectral correlates to printer digital counts. Finally, this research has shown the analysis of spectral redundancy within a printer can be applied to the fields of image security and steganography. The methods developed to uncover spectral redundancy can be used to make an embedded image visually detectable by having ink sets with various gloss characteristics. If an ink set has similar gloss characteristics, and the inks are highly spectrally redundant, it is possible to embedded an image so that it is completely undetectable.

The new concepts developed and implemented in this research are very important to the spectral imaging community. Hopefully this research will inspire many topics in the area of spectrally stable multi-ink variability.

REFERENCES

- ¹ D. Tzeng, Spectral-Based Color Separation Algorithm Development for Multiple-Ink Color Reproduction, *Ph.D Dissertation*, RIT 1999.
- ² L. Taplin, and R. Berns, Spectral Color Reproduction Based on a Six-Color Inkjet Output System, *Proc. of Ninth Color Imaging Conference*, pp. 209-213. (2001).
- ³ F. Imai, M. Rosen, D. Wyble, R. Berns, and D. Tzeng, Spectral Reproduction from Scene to Hardcopy I: Input and Output, *Proc. of SPIE*, **4306**, pp. 346-357. (2001).
- ⁴ M. Rosen, F. Imai, X. Jiang, and N. Ohta, Spectral Reproduction from Scene to Hardcopy II: Image Processing, *Proc. of SPIE*, **4300**, pp. 33-41. (2001).
- ⁵ M. Rosen, L. Taplin, F. Imai, R. Berns, and N. Ohta, Answering Hunt's Web Shopping Challenge: Spectral Color Management for a Virtual Swatch, *Proc. of Ninth Color Imaging Conference*, pp. 267-273. (2001).
- ⁶ K. Iino and R. Berns, Building Color Management Modules Using Linear Optimization I. Desktop Color System, *J. Imaging Sci. Tech.* **42**, 79-94. (1998).
- ⁷ K. Iino and R. Berns, Building Color Management Modules Using Linear Optimization II. Prepress System For Offset Printing, *J. Imaging Sci. Tech.* **42**, 99-144. (1998).
- ⁸ D. Wyble and R. Berns, A Critical Review of Spectral Models Applied To Binary Color Printing, *Color Res. Appl.* **25**, 4-15. (2000).
- ⁹ M. Rosen and X. Jiang, Lippmann2000: A Spectral Image Database Under Construction, *Proc. of the International Symposium on Multispectral Imaging and Color Reproduction for Digital Archives*, Chiba University, Chiba, Japan, pp. 117-122. (1999).
- ¹⁰ R. Berns, and M. Shyu, Colorimetric Characterization of A Desktop Drum Scanner Using A Spectral Model, *J. Electronic Imaging.* **4**, 360-372. (1995).
- ¹¹ M. Rosen, E. Hattenberger, and N. Ohta, Spectral Redundancy in A 6-Ink Inkjet Printer, *Proc. of PICS*, pp. 236-243. (2003).
- ¹² H. Kang, Color Technology for Electronic Imaging Devices, SPIE Press, Bellingham (1997).
- ¹³ F. Imai, M. Rosen, and R. Berns, Comparative Study of Metrics for Spectral Match Quality, *Proc. of First European Conference on Colour in Graphics, Imaging and Vision*, pp. 492-496. (2002).

- ¹⁴ J. Hernández-Andrés and J. Romero, Colorimetric And Spectroradiometric Characteristics of Narrow-Field-of-View-Clear Skylight in Granada, Spain, *JOSA A*, **18** pp. 412-420. (2001).
- ¹⁵ J. B. Cohen, Visual Color and Color Mixture, University of Illinois Press, 2001.
- ¹⁶ J. Fridrich, M. Goljan, Practical Steganalysis of Digital Images – State of the art, *Proc. of SPIE*, **4675**, pp. 1-13. (2002).
- ¹⁷ S. Wang, K. Knox, Embedding Digital Watermarks In Halftone Screens, *Proc. of SPIE*, **3971**, pp. 218-227. (2000).
- ¹⁸ M. Fu, O. Au, Data Hiding For Halftone Images, *Proc. of SPIE*, **3971**, pp. 228-236. (2000).
- ¹⁹ H. Kim, H-K. Lee, H-Y. Lee, Y. Ha, Digital Watermarking Based On Color Differences, *Proc. of SPIE*, **4314**, pp. 10-17. (2001).

APPENDIX A. MATLAB CODE

A-1 Printer Model.

```
% One piece LUT.
function R_predicted = fwdLUT(a,LUTparameters)
a=flipr(a);

% Find the side of the center.
b=find(a>1);
a(b)=1;

p = sum(ones(size(LUTparameters.node_ac_levels,1)-1,1)*a...
    > LUTparameters.node_ac_levels(2:size(LUTparameters.node_ac_levels,1),:),1);

% Find the adjacent digital count primaries
h_ac=zeros(1,6);
l_ac=zeros(1,6);
for i=1:6
    h_ac(i)=LUTparameters.node_ac_levels(2+p(i),i);
    l_ac(i)=LUTparameters.node_ac_levels(1+p(i),i);
end

% Compute the local area coverages
b = (a-l_ac)./(h_ac-l_ac);

% Find offsets for the list of primaries
list = (ones(64,1)*p+LUTparameters.dmask)*(LUTparameters.node_levels.^[0:5])+1;

% Convert all zeros back to paper reflectance.
if find(list==0)
    list(find(list==0))=1
end

% Check if any primaries missing.
list_ac = LUTparameters.node_ac(:,list);
ac_result=length(find(isnan(list_ac)));
if ac_result(1) == 0
    area = ones(2^LUTparameters.inks,1)*b;
    R_predicted = (LUTparameters.node_refl(:,list)*...
        prod(area.*LUTparameters.dmask + (1-area).*~LUTparameters.dmask,2));
else
    R_predicted = ones(31,1)*-1;
end
```

A-2 Spectrally stable multi-ink variability algorithm.

```
function CMYKGO_RMS = inverse_model(cmykgo_ac,spectra_measured,LUTchar)
options = optimset('Diagnostics','off','Display','off','Tolfun',1e-4,...
    'MaxFunEvals',2000,'MaxIter',2000);
warning 'off'
```

```

global cmykgo;
cmykgo = zeros(1,6);

CMYKGO_RMS = zeros(6,256,7);
ub = ones(1,6);
lb = zeros(1,6);
% convert area coverages to digital counts.
dc = zeros(size(cmykgo_ac));
dc(1) = round(interp1(LUTchar.ramp_LUT(1,:),[0:255],cmykgo_ac(1)));
dc(2) = round(interp1(LUTchar.ramp_LUT(2,:),[0:255],cmykgo_ac(2)));
dc(3) = round(interp1(LUTchar.ramp_LUT(3,:),[0:255],cmykgo_ac(3)));
dc(4) = round(interp1(LUTchar.ramp_LUT(4,:),[0:255],cmykgo_ac(4)));
dc(5) = round(interp1(LUTchar.ramp_LUT(5,:),[0:255],cmykgo_ac(5)));
dc(6) = round(interp1(LUTchar.ramp_LUT(6,:),[0:255],cmykgo_ac(6)));

start_ac = zeros(1,5);
for ink = 1:6
    % Define the starting values.
    if ink > 1
        start_ac(1:ink-1) = cmykgo_ac(1:ink-1);
    end
    if ink < 6
        start_ac(ink:5) = cmykgo_ac(ink+1:6);
    end

    start_ac = start_ac + 0.0001;

    for ctrl_dc = dc(ink):255 % Runs from ink DC to 255.
        ctrl_ac = interp1([0:255],LUTchar.ramp_LUT(ink,:),ctrl_dc);

        % Define the upper and lower bounds.
        [result_ac,CMYKGO_RMS(ink,ctrl_dc+1,1)] = fmincon(@rms_obj2,...
            [start_ac,[],[],[],[],[lb],[ub],[],...
            options,LUTchar,spectra_measured,ink,ctrl_ac);

        start_ac = result_ac;

        if ink > 1
            CMYKGO_RMS(ink,ctrl_dc+1,2:ink) = result_ac(1:ink-1);
        end
        CMYKGO_RMS(ink,ctrl_dc+1,ink+1) = ctrl_ac;
        if ink < 6
            CMYKGO_RMS(ink,ctrl_dc+1,2+ink:7) = result_ac(ink:5);
        end
    end
end
%%%%%%%%%%%%%%%%%%%%%%%%%%%%%%%%%%%%%%%%%%%%%%%%%%%%%%%%%%%%%%%%%%%%%%%%
if ink > 1
    start_ac(1:ink-1) = cmykgo_ac(1:ink-1);
end
if ink < 6
    start_ac(ink:5) = cmykgo_ac(ink+1:6);
end

for ctrl_dc = fliplr(0:dc(ink)-1) % Runs from ink DC to 255.
    ctrl_ac = interp1([0:255],LUTchar.ramp_LUT(ink,:),ctrl_dc);

```

```

% Define the upper and lower bounds.
[result_ac,CMYKGO_RMS(ink,ctrl_dc+1,1)] = fmincon(@rms_obj2,...
    [start_ac,[],[],[],[],[lb],[ub],[],...
    options,LUTchar,spectra_measured,ink,ctrl_ac);

start_ac = result_ac;

if ink > 1
    CMYKGO_RMS(ink,ctrl_dc+1,2:ink) = result_ac(1:ink-1);
end
CMYKGO_RMS(ink,ctrl_dc+1,ink+1) = ctrl_ac;

if ink < 6
    CMYKGO_RMS(ink,ctrl_dc+1,2+ink:7) = result_ac(ink:5);
end
end
end
end

```

A-3 Code to create density maps for the midpoint dataset.

```

% Load the midpoint data.
load mdpts.mat;

% Colorimetric data.
cmf = load('2degCMF400_700_10nm.txt');
D65 = load('D65_400_700_10nm.txt');
A = load('A_400_700_10nm.txt');
XYZD65 = spectra_to_xyz(mdpts.refl,cmf,D65);

% Define the spectral tolerance.
err_tol = 0.02;

%This determines the distance in area coverage from the original value.
load ac_start_index_mdpt.mat;

% Determine the max ac distance and range for each midpoint.
mdpt_vis = zeros(6,2,4096);
for ink = 1:6
    for mdpt = 1:4096
        ii = find(mdpts.results(ink,:,1,mdpt) <= err_tol);
        ac_distance = ac_start_index_mdpt(ink,ii,mdpt);
        mdpt_vis(ink,1,mdpt) = ac_distance(1) + ac_distance(end);%range.
        mdpt_vis(ink,2,mdpt) = max(ac_distance);%max dc dist.
    end
end
mdpt_vis(find(mdpt_vis > 1)) = 1;

%%%%%%%% Spectral 6-D analysis. %%%%%%%%%

% Reshape and place into correct matrix.
Y_range = reshape(squeeze(XYZD65(2,:)),64,64);
orig_ac = reshape(mdpts.ac,64,64,6);
range = reshape(squeeze(mdpt_vis(:,1,:)),6,64,64);

```

```

maximum = reshape(squeeze(mdpt_vis(:,2,:)),6,64,64);

% Redefine the colormap for improved differentiation.
my_map = jet(256);
my_map_lut = zeros(7,3);
my_map_lut(1,:) = [0 0 .20];
my_map_lut(2,:) = [0 0.51562 1];
my_map_lut(3,:) = [0.015625 1 0.98438];
my_map_lut(4,:) = [0.51562 1 0.48438];
my_map_lut(5,:) = [1 1 0];
my_map_lut(6,:) = [1 .5 0];
my_map_lut(7,:) = [1 0 0];

%%%%%%%%%%%%%%%%%%%%%%%%%%%%%%%%%%%%%%%%%%%%%%%%%%%%%%%%%%%%%%%%%%%%%%%%
% Plot the 6-D data in 3-D via slice. 4 graphs for each color.
colors = {'cyan','magenta','yellow','black','green','orange'};
for ink = 1:length(colors)
    r = squeeze(range(ink,:,:));
    a = 12.5;
    for j = 1:16:64
        r2 = reshape(r(:,j:j+15),16,4,16);
        %[Xi,Yi,Zi] = ndgrid([1:17],[1:17],[87.5 62.5 37.5 12.5]);
        [Xi,Yi,Zi] = meshgrid(fliplr([1:17]),[1:17],[.875 .625 .375 .125]);
        rand('state',0);
        h = figure;slice(Xi,Yi,Zi,rand(17,17,4),[],[],[.875 .625 .375 .125],'nearest');
        h2 = findobj(h,'Type','Surface');
        colormap(my_map_lut);
        h3 = colorbar('vert');
        for k=1:4 %plot each slice.
            set(h2(k),'cdata',squeeze(r2(:,k,:)),'FaceColor','TextureMap');
            %set(h2(j),'FaceAlpha',0.5); for transparency
        end
        if j == 49;
            h3 = colorbar('vert');
            set(h3,'YTickLabel',[0:.15:1 1],'YLim',[0 1],'YTick',...
                [0:7]/7);
        else
            h3 = colorbar('vert');
            set(h3,'Visible','off');
        end
        end
        axis([0 17 0 17 0 1]);
        view([166 14]);
        h4 = zlabel('Black Fractional Area Coverage');set(h4,'FontSize',[16]);
        h4 = ylabel('O G');set(h4,'FontSize',[16]);
        h4 = xlabel('Y M');set(h4,'FontSize',[16]);
        h4 = title(sprintf('Variability of %s for cyan at %g%% area coverage.',colors{ink},a));
        set(h4,'FontSize',[16]);
        a=a+25;
    end
end
end

```

A-4 Code to create density maps for the LUT node factorial sampling.

```
% Load the LUTnode data.
load LUT051.mat;
load LUTchar.mat;

% Colorimetric data.
cmf = load('2degCMF400_700_10nm.txt');
D65 = load('D65_400_700_10nm.txt');
A = load('A_400_700_10nm.txt');
XYZD65 = spectra_to_xyz(LUT_out.refl,cmf,D65);

% Define the error tolerance
err_tol = 0.02;
% Determine the image dimension for each axis.
dim = sqrt(size(LUT_out.redundancy,4));

%This determines the distance in area coverage from the original value.
load ac_start_idx_LUT051.mat;

% Determine the max ac distance and range for each LUT node.
vis = zeros(6,2,size(LUT_out.redundancy,4));
for ink = 1:6
    for patch = 1:size(LUT_out.redundancy,4)
        ii = find(LUT_out.redundancy(ink, :, 1, patch) <= err_tol);
        ac_distance = ac_start_idx_LUT051(ink,ii,patch);
        vis(ink,1,patch) = ac_distance(1) + ac_distance(end);%range.
        vis(ink,2,patch) = max(ac_distance);%max dc dist.
    end
end
vis(find(vis > 1)) = 1;

%%%%%%%%% Spectral 6-D analysis. %%%%%%%%%%

% Reshape and place into correct matrix.
Y_range = reshape(squeeze(XYZD65(2,:)),dim,dim);
orig_ac = reshape(LUT_out.ac,dim,dim,6);
range = reshape(squeeze(vis(:,1,:)),6,dim,dim);
maximum = reshape(squeeze(vis(:,2,:)),6,dim,dim);

% Redefine the colormap for improved differentiation.
my_map = jet(256);
my_map_lut = zeros(7,3);
my_map_lut(1,:) = [0 0 .20];
my_map_lut(2,:) = [0 0.51562 1];
my_map_lut(3,:) = [0.015625 1 0.98438];
my_map_lut(4,:) = [0.51562 1 0.48438];
my_map_lut(5,:) = [1 1 0];
my_map_lut(6,:) = [1 .5 0];
my_map_lut(7,:) = [1 0 0];

%%%%%%%%%

% Plot the 6-D data in 3-D via slice. 4 graphs for each color.
colors = {'cyan','magenta','yellow','black','green','orange'};
for ink = 1:length(colors)
```

```

r = squeeze(range(ink,:,:));
a = 0;
for j = 1:9:27
    r2 = reshape(r(:,j:j+8),9,3,9);
    %[Xi,Yi,Zi] = ndgrid([1:17],[1:17],[87.5 62.5 37.5 12.5]);
    [Xi,Yi,Zi] = meshgrid(fliplr([1:10]),[1:10],[1 .5 0]);
    rand('state',0);
    h = figure;slice(Xi,Yi,Zi,rand(10,10,3),[],[],[1 .5 0],'nearest');
    h2 = findobj(h,'Type','Surface');
    colormap(my_map_lut);
    h3 = colorbar('vert');
    for k=1:3 %plot each slice.
        set(h2(k),'cdata',squeeze(r2(:,k,:)),'FaceColor','TextureMap');
        %set(h2(j),'FaceAlpha',0.5); for transparency
    end
    if j == 19;
        h3 = colorbar('vert');
        set(h3,'YTickLabel',[0:.15:1 1],'YLim',[0 1],'YTick',...
            [0:7]/7);
    else
        h3 = colorbar('vert');
        set(h3,'Visible','off');
    end

    axis([0 10 0 10 0 1]);
    view([166 14]);
    h4 = xlabel('Black Fractional Area Coverage'); set(h4,'FontSize',[16]);
    h4 = ylabel('O G'); set(h4,'FontSize',[16]);
    h4 = xlabel('Y M'); set(h4,'FontSize',[16]);
    h4 = title(sprintf('Variability of %s for cyan at %g%% area coverage.',colors{ink},a));
    set(h4,'FontSize',[16]);
    a=a+50;
end
end
end

```

A-5 Level 1: Embedding Information In A Uniform Color Patch

```

% Read in the image.
image = imread('EXPT1_MCSL.bmp');
ink_array = zeros(1232*3000,6);

% Two spectrally similar ink combinations.
combo1 = [24 5 3 0 218 3];
combo2 = [0 13 0 0 255 0];

% Assign different ink combo's to according areas.
ii = find(image == 1);
for i = 1:6
    ink_array(ii,i) = combo1(i);
end

ij = find(image == 0);
for j = 1:6
    ink_array(ij,j) = combo2(j);
end

```

```

end

ink_array = reshape(ink_array,1232,3000,6);
ink_array = 255 - ink_array;
ink_array = ink_array/255;

% Save individual channels.
colors = 'CMYKGO';
for i=1:6
    sprintf('Working on MCSL_%s tiff file.',colors(i))
    imwrite(ink_array(:,:,i),sprintf('MCSL_%s.tif',colors(i)), 'Resolution',300);
end

```

A-6 Level 2: Simple Image Watermarking

```

% Read in the image.
hidden = imread('EXPT1_MCSL.bmp');
image = imread('EXPT22_MCSL.tif');
ink_array = zeros(1232*3000,6);

% Twelve spectrally similar ink combinations.
%dc_o = ac2dc(mdpts.ac(1797,:),LUTchar)
%dc_m = ac2dc(squeeze(mdpts.results(5,1,2:7,1797)),LUTchar)
% Level 1 "Greenish Color" Mdpt 2249 - Green Distance.
combo1a = [61 6 186 3 83 5];
combo1b = [91 0 199 1 48 9];
% Level 2 "Reddish Color" Mdpt 780 - Green Distance.
combo2a = [7 131 11 3 83 126];
combo2b = [14 93 12 14 48 150];
% Level 3 "Dark Grayish Color" Mdpt 1291 - Green Distance
combo3a = [26 22 11 3 83 51];
combo3b = [51 12 16 3 48 58];
% Level 4 "Bluish Color" Mdpt 2057 - Green Distance
combo4a = [61 6 11 3 83 5];
combo4b = [89 2 19 0 48 10];
% Level 5 "Brownish Color" Mdpt 476 - Green Distance
combo5a = [7 22 186 11 83 126];
combo5b = [31 1 253 12 48 145];
% Level 6 "Purpleish Color" Mdpt 1802 - Green Distance.
combo6a = [26 131 11 3 83 21];
combo6b = [50 131 19 3 48 17];

mdpt = [combo1a;combo2a;combo3a;...
        combo4a;combo5a;combo6a];
mdpt_match = [combo1b;combo2b;combo3b;...
              combo4b;combo5b;combo6b];

% Assign different ink combo's to according areas.
% The quantized levels are 0 51 102 153 204 255 dc.

% Assign spectrally similar midpoints to "on" binary image.
j = [0 51 102 153 204 255];
for i = 1:6
    ii = find((hidden == 1) & (image == j(i)));

```

```

    for k = 1:6
        ink_array(ii,k) = mdpt_match(i,k);
    end
end

% Assign midpoints to "off" binary image.
for i = 1:6
    ii = find((hidden == 0) & (image == j(i)));
    for k = 1:6
        ink_array(ii,k) = mdpt(i,k);
    end
end

% Invert image and scale between 0 and 1.
ink_array = reshape(ink_array,1232,3000,6);
ink_array = 255 - ink_array;
ink_array = ink_array/255;

% Save individual channels.
colors = 'CMYKGO';
for i=1:6
    sprintf('Working on MCSL22_%s tiff file.',colors(i))
    imwrite(ink_array(:, :, i), sprintf('MCSL22_%s.tif',colors(i)), 'Resolution', 300);
end

```

A-7 Level 3: Complex Image Watermarking

```

%Load midpoint information.
%load mdpts.mat;
load LUTchar;

% Select channel to hide hidden image.
channel = 5;

% Load the hidden image.
hidden = 255-double(imread('rosetta_gray.tif'));

% Load the mandrill.
load mandrill_ac_dc.mat;

% Reshape the visible and hidden images.
hidden = reshape(hidden,size(hidden,1)*size(hidden,2),1);
visible = dc2ac(255-double(reshape(img_dc,512*512,6)),LUTchar);

% Algorithm to assign associated CMYKGO based on hidden image.
% Creates a sub index of the midpoint area coverages (0,1,2,3).
vis_sub = fix(visible*4)-(visible==1);

% change from 6 base 4 digits to one base 10 number for index into midpoint array using the info in the
hidden image.
vis_idx = ones(size(vis_sub,1),1);
for i = 1:6
    vis_idx = vis_idx + (vis_sub(:,i))*4.^(6-i);
end

```

```

vis_idx2 = sub2ind([256,4096],hidden+1,vis_idx);

% Put hidden image in a specific channel.
LUT = squeeze(mdpts.results(channel,:,:));

% Algorithm that does not allow spectral error at eachpixel to go above 0.02 RMS.
for i = 1:4096
    good = find(LUT(:,1,i) <= 0.02);
    lo = LUT(good(1),:,i);
    hi = LUT(good(end),:,i);
    bad = find(LUT(:,1,i) > 0.02);
    if ~isempty(bad)
        if good(1) > bad(1)
            LUT(1:good(1)-1, :, i) = ones(size(LUT(1:good(1)-1, :, i))) * diag(lo);
        end
        if good(end) < bad(end)
            LUT(good(end)+1:end, :, i) = ones(size(LUT(good(end)+1:end, :, i))) * diag(hi);
        end
    end
end
LUT = permute(LUT,[1,3,2]);
LUT = reshape(LUT,256*4096,7);
image_out = LUT(vis_idx2,2:7);

% change from 6 base 4 digits to one base 10 number for index into midpoints using quantized image.
o_image_out = mdpts.ac(vis_idx,:);

% Convert ac to dc for original quantized and watermarked image.
image_out = 255 - ac2dc(image_out,LUTchar);
o_image_out = 255 - ac2dc(o_image_out,LUTchar);

% Reshape images.
image_out = reshape(image_out,size(img_ac,1),size(img_ac,2),6);
o_image_out = reshape(o_image_out,size(img_ac,1),size(img_ac,2),6);

% Write the 6 tiff files for original image.
colors = 'CMYKGO';
for i=1:6
    sprintf('Working on mandrill_orig_%s tiff file.',colors(i))
    imwrite(uint8(o_image_out(:, :, i)),sprintf('mandrill_orig_%s.tif',colors(i)), 'Resolution',300);
end

% Write the 6 tiff files for the watermarked image.
for i=1:6
    sprintf('Working on mandrill_water_%s tiff file.',colors(i))
    imwrite(uint8(image_out(:, :, i)),sprintf('mandrill_water_%s.tif',colors(i)), 'Resolution',300);
end

```

**APPENDIX B. SPECTRALLY REDUNDANT MIDPOINT
SAMPLES**

**APPENDIX C. SPECTRALLY REDUNDANT LUT NODE
SAMPLES**

**APPENDIX D. SPECTRALLY REDUNDANT MIDPOINT
SAMPLES USED IN SPECTRAL ERROR METRIC
INVESTIGATION**

**APPENDIX E. SAMPLES EXHIBITING INTERPOLATION
ERRORS BETWEEN NODES**

**APPENDIX F. SPECTRALLY TRANSLUCENT
WATERMARKING EXAMPLES**

Level 1: Embedding Information In A Uniform Color Patch

Pages F-3 – F-4

Page F-3: Watermarked Image

Page F-4: Ink Separations

Level 2: Simple Image Watermarking

Pages F-5 – F-6

Page F-5: Watermarked Image

Page F-6: Ink Separations

Level 3: Complex Image Watermarking

Pages F-7 – F-10

Page F-7: Original Image (Left), Watermarked Image (Right)

Page F-8: Ink Separations – Cyan (Left), Magenta (Right)

Page F-9: Ink Separations – Yellow (Left), Black (Right)

Page F-10: Ink Separations – Green (Left), Orange (Right)

Watermarked Image

Watermarked Image

Watermarked Image

Original Image

Magenta

Cyan

Black

Yellow

Orange

Green